Wireless Baseband Transmission
– Proposal and Experiments of a New Wireless Transmission Scheme

Jun-ichi Kitagawa

The University of Electro-Communications

Dec. 2006

Wireless Baseband Transmission – Proposal and Experiments of a New Wireless Transmission Scheme

Jun-ichi Kitagawa

Graduate School of Electro-Communications,
The University of Electro-Communications

PhD Thesis
Dec. 2006

Wireless Baseband Transmission
– Proposal and Experiments of a New Wireless Transmission Scheme

Approved by Supervisory Committee:

Chairperson: Prof. Yoshio Karasawa

Member: Prof. Takeshi Hashimoto

Member: Prof. Masashi Hayakawa

Member: Prof. Takashi Iwasaki

Member: Prof. Kazuhiko Honjo

WBT（無線ベースバンド伝送）
— 新しい無線伝送方式の提案と実験

北川 淳一

電気通信大学 大学院電気通信学研究科

概要

Wireless Baseband Transmission (WBT) という新しい無線伝送方式を提案し，実験によってその基礎的特性を調べている．一般に伝送システムは，送りたい情報をそのまま何らかの物理的信号に対応付けて送信するベースバンド伝送方式と，搬送波と呼ばれる信号を送りたい情報によって変調して送信する搬送伝送方式の 2 つに分けることができる．これまで無線伝送の分野においては搬送伝送方式のみが用いられてきた．それに対し，有線伝送においてはベースバンド伝送，搬送伝送共に利用されている．本研究は無線でもベースバンド伝送が可能かどうかを検討したものであるということができる．実験をおこなった結果，適切なアンテナ（本研究ではディスコーンアンテナ）と伝送路符号化（本研究では Manchester 符号化）を用いればベースバンド伝送を無線でおこなうことも可能であることが明らかになった．

本論文は 1 章から 8 章までの構成である．

1 章ではこれまでの無線伝送について歴史を踏まえて記述している．

2 章では WBT の概念について WBT と比較的似ているシステムである Impulse Radio との比較も含めて述べている．

3 章では BER（bit error rate）を計算するための実信号解析法について述べている．実信号解析法は，WBT では一般の無線伝送で用いられている等価低域系による複素領域での表現はできずに，全て実信号として取り扱う必要があることを述べたものであり，従来の無線伝送の解析と異なる点である．

4 章では WBT の時間領域における伝送実験と周波数領域での測定（100 MHz）と 3 章の手法を組み合わせた解析，5 章では周波数領域における測定（1 GHz）と 3 章の手法を組み合わせた解析について述べている．実験は全て本学の電波暗室内でおこない，自由空間と人工的に作り出したマルチパス環境下について伝送特性の評価をおこなっている．その評価の指標として BER を用いている．また，チャネルの周波数特性やインパルス応答についても示している．さらに，時間領域と周波数領域での測定が一致することも示している．

5 章では 3 章と 4 章の結果を利用し周波数領域でのみ測定をおこなっている．一般に時間領域測定に比べ周波数領域測定は高い周波数まで対応可能であり，これは小型アンテナの使用ができることを意味する．測定の容易さと効率を考えると周波数領域でのみ測定しても時間領域測定と同じ結果が得られることは有益な結果であるといえる．

6 章では 4 章と 5 章で得られた結果を基にして，送受信に無指向性アンテ

ナを用いた場合における WBT の簡単な伝送モデルである-6 dB/octave モデルを示している．このモデルを使用して仮想的なアンテナ帯域幅の下限周波数，上限周波数，比帯域を変化させて BER 特性を求めている．この結果は実際の WBT 無線システムを実現するにあたり必要となる情報伝送レートとアンテナ帯域幅との関係について有意な情報を与える．また，チャネルの等化についてもふれ，さらに各種直流平衡符号に対する BER 特性の比較もおこなっている．

7 章では WBT の応用について述べている．具体的には WBT 無線機の構成，近傍界通信への適用，さらに MIMO(multiple input multiple output) や SDR(software defined radio) といった近年無線通信の世界で話題になっているシステムについて WBT の関わりを述べている．

8 章では結論を述べている．すなわち，WBT という新たな伝送方式を提案し，有線のみならず無線でもベースバンド伝送は可能であることを実験によって明らかにしたことを記述している．

Abstract

A baseband transmission scheme for wireless communications has been proposed and examined. The *wireless baseband transmission (WBT)* scheme radiates a baseband signal stream, such as non-return-to-zero (NRZ), return-to-zero (RZ), or Manchester encoded signals, directly from an antenna. Namely, a carrier in terms of a sinusoidal radio wave or light wave is not used in the transmission. In experiments, baseband signals generated with a data generator are radiated directly from a discone antenna, and received waveforms are observed with a digital storage oscilloscope (DSO). The experiments show that WBT is realisable when using antennas with a flat amplitude spectrum and a linear phase characteristic, such as discone antennas, over a given band.

WBT experiments in frequency-domain are also carried out using a vector network analyser (VNA). Same results are obtained in the time-domain (using a DSO) and frequency-domain (using a VNA) measurements. Bit-error-rate (BER) characteristics are calculated using channel characteristic data taken by a VNA. Manchester encoding is superior in BER to NRZ and RZ. BER characteristics are given both in free-space and multipath environments. Treating WBT signals on a computer, we have to consider a WBT signal as a real signal not a complex

signal. We can not treat a WBT signal in the equivalent low-pass system which is used commonly in wireless systems. Because the equivalent low-pass system assumes a passband type signal with narrow fractional bandwidth. Therefore, a signal analysis method for WBT is required to evaluate transmission characteristics. BER characteristics in this paper are calculated using channel characteristics taken by a VNA and a computer. We have confirmed a 250 Mbps and 2.5 Gbps data transmissions of WBT in the time-domain and frequency-domain, respectively. A dominant factor for WBT in multipath environments is the ratio between the power of a direct wave and that of reflected waves not the number of passes.

Although we do not suppose specific applications for this WBT, considering practical application systems, this system might be a candidate for the effective use of millimetre or sub-millimetre wave regions, which have extremely wide bandwidths for high-speed (e.g., 100 Gbps) wireless transmissions. Furthermore, interference problems are mitigated in these regions because millimetre electromagnetic waves are attenuated rapidly in the atmosphere by water vapour and oxygen. The present system might also be applicable to communication systems using near electromagnetic-fields, although we treat only far one in the present paper. At least at present, actual operation would be limited to special environments in which there is no need to take interference problems into account. However, we believe that WBT is to be a candidate for a new wireless transmission scheme.

Contents

List of Figures

Chapter 1

Introduction

1.1 Motivation

This paper presents a baseband [1] transmission scheme for wireless communications which is fundamentally different from conventional wireless transmission schemes. The scheme, which we call *wireless baseband transmission*, radiates a baseband signal stream, such as non-return-to-zero (NRZ), return-to-zero (RZ), or Manchester encoded signals, directly from an antenna. Namely, a carrier in terms of a sinusoidal radio wave or light wave is not used in the transmission. We propose a new wireless transmission scheme and investigate experimentally the feasibility of a baseband transmission for wireless communications for the purpose of finding a new wireless transmission scheme.

[1] In this paper, we define the term *baseband* as the square waveform which indicates information itself and any sinusoidal waves are not used in the transmission.

1.2 Transmission Systems in Electrical Communications

There are two schemes used in transmission systems. One is carrier transmission (or passband transmission), and the other is baseband transmission. Wireless transmissions adopt carrier transmission systems almost exclusively, although both baseband and carrier transmission systems are used in wired transmissions. Conventional wireless transmission systems, i.e., carrier transmission systems, modulate a carrier with a baseband signal of a message source to raise affinities for a communication channel including antennas. A typical carrier is a sinusoidal electromagnetic wave. There are two main reasons for the modulation. First, baseband signals could not be radiated efficiently from antennas because they have low-frequency components. Second, it is possible to use frequency division multiplexing (FDM) schemes which shift the signal spectrum.

1.3 From Conventional Wireless Systems to WBT

Recently, a large number of people are using a variety of wireless communications equipment. The trend in wireless communications has been toward digital communications from analogue communications with the progress of computer technologies. To increase the data transmission speed, the pulse width of the baseband data signal has become shorter and shorter. Consequently, the required carrier frequency increases in proportion to the baseband data signal bandwidth, which depends on the amount of information sent in the transmission. Since the fractional bandwidth for a typical wireless system is less than 5%, for example, assuming that the transmission of information at a rate of more than 10 Giga-symbol/s, signals having a carrier frequency of approximately THz frequency is needed. This falls within the range of optical wireless communication.

However, when we consider the information signal bandwidth, we might expect that such a baseband signal propagates by its own ability without a carrier. Therefore, we come by the idea that the original information itself is directly transmitted from an antenna without the need for modulation techniques [1]. This is the concept of the wireless baseband transmission examined herein. This system could also be expressed as a system in which baseband transmissions used in wired transmissions are applied to wireless transmissions. Because baseband data signals are radiated directly, an extremely wide bandwidth is occupied. Hence, it is presumed that the coexistence with other wireless systems becomes an important problem. This problem also appears in application systems of ultra-wide-band (UWB[2]) technologies [2–8]. However, we carried out wireless baseband transmission experiments because we would like to investigate the fundamental capabilities and characteristics of this scheme. Although we do not suppose specific applications for this wireless baseband transmission scheme, considering practical application systems, this system might be a candidate for the effective use of millimetre or sub-millimetre wave regions, which have extremely wide bandwidths for high-speed (such as 100 Gbps) wireless transmissions. Furthermore,

[2]We use the term UWB in a broad sense in the present paper, i.e., UWB does not indicate a specific application or product.

interference problems are mitigated in these regions because millimetre electromagnetic waves are attenuated rapidly in the atmosphere by water vapour and oxygen, for example. The present system might also be applicable to communication systems using near electromagnetic-fields, although we treat only far one in this paper.

1.4 Historical Perspectives of Wireless Communications

Wireless (Radio) technologies have a history for over one century. It has its origin in the work of J. C. Maxwell. The contribution is known as Maxwell's equations. The equations are appeared in 1864 and the relationship between electromagnetic and magnetic fields is described elegantly in the equations. Although Maxwell's equations state the existence of electro-magnetic waves theoretically, no one had verified the existence experimentally. In 1888, H. R. Hertz verified the existence experimentally using ultra high frequency (UHF) electro-magnetic waves. G. Marconi is also known as a pioneer of wireless technologies. He succeeded a long distance wireless communication across the Atlantic between Poldhu, Cornwall, and St. John's, Newfoundland in 1901. This event made wireless communications more practical. Long electromagnetic waves were used at the beginning of wireless communications because such waves were considered to be able to propagate for a long distance. In the early wireless communications, impulse like electromagnetic waves by sparks were used to transform information. R. A. Fessenden succeeded in transmitting voice by sparks in 1901. This is the first *modulation* and the fundamental scheme of wireless transmissions has not been changed for over 100 years. We will try to make a breakthrough in this paper. More detailed description is shown in the history references, e.g., Ref. [9].

1.5 Outline of this paper

This paper is organised as follows. The concept of WBT is explained in Chapter 2. A baseband signal analysis method for WBT is given in Chapter 3. This point is different from conventional signal analysis of wireless systems; i.e., WBT signal analysis is not performed in the equivalent low-pass system which is commonly used and written using complex numbers. WBT transmission experiments are described in Chapter 4 and Chapter 5. A WBT transmission model for designing WBT systems is described in Chapter 6. Other WBT topics, transceiver architecture, near electromagnetic-fields communications, MIMO (multiple input multiple output), and SDR (software defined radio) are given in Chapter 7. Finally, the conclusion of this study is described in Chapter 8.

Chapter 2

Concept of WBT

2.1 Origin

When we pay attention to the information signal bandwidth of several Gbps, we can expect that such a baseband signal propagates by its own ability without a carrier. Therefore, the idea is born that original information itself is directly transmitted from an antenna without modulation techniques [1]. That is the concept of the WBT. This system can also be expressed as a system applying baseband transmissions used in wired transmissions to wireless transmissions. Because baseband data signals are radiated directly, an extremely wide bandwidth is occupied. Hence, it is presumed that the coexistence with other wireless systems becomes an important problem. This problem is also appeared in application systems of ultra-wide-band (UWB[1]) technologies [2–8]. However, we carried out WBT experiments because we would like to investigate the fundamental capabilities and characteristics. Although we do not suppose specific applications of

[1]We use the term 'UWB' in a wide sense in this paper; i.e., not pointing to a specific application or product.

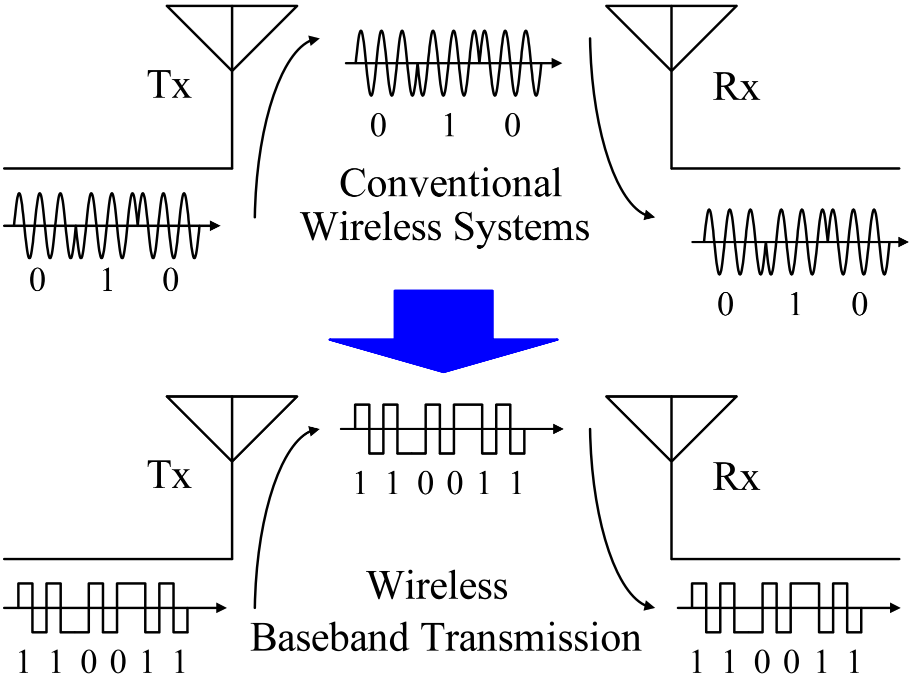

Fig. 2.1 Concept of WBT

this wireless baseband transmission for that reason, still considering practical application systems, this system might be a candidate for effective use of millimetre or sub-millimetre wave regions, which have extremely wide bandwidths for high-speed (such as 100 Gbps) wireless transmissions. Furthermore, interference problems are mitigated in that regions because millimetre electromagnetic waves are attenuated rapidly in the atmosphere by water molecules etc. Such a communication using near electromagnetic-fields might also be suitable as application systems of this system although we treat only far electromagnetic-fields in this paper. Figure 2.1 shows the concept of WBT. As shown in Fig. 2.1, a baseband signal is transmitted directly from an antenna in WBT.

2.2 Impulse Radio (IR) and UWB

We consider wireless systems which do not use a carrier wave. A similar system to this wireless baseband transmission one is known as impulse radio (IR) [10,11]. IR radiates a pulse so-called Gaussian mono-cycle which has nano-second order duration. It uses modulation techniques such as pulse position modulation (PPM) for the transmission of information. It is required, therefore, a bit of special pulse generator circuits and modulation ones. On the other hand, WBT requires only a simple waveform generator which is capable of making a general transmission waveform used in wired communications. Because we can regard WBT as one of waveform transmissions, it is required to transmit the shape of a waveform itself faithfully.

2.2.1 A Brief History of UWB Communications

We investigated UWB communications history to distinguish our transmission scheme from other UWB technologies. The origin of UWB technologies began with time-domain electromagnetics in 1960s [13]. It is difficult to separate UWB technologies from radar technologies, and really radar was one of the major applications of time-domain electromagnetics at the beginning of that. Considering the aspect of communications, there are two pioneers in UWB communications. One is G. F. Ross and the other is H. F. Harmuth as explaining in the next paragraph. As a matter of fact, both Ross and Harmuth have contributions not only to UWB communication technologies but to UWB radar technologies, however, we feature only UWB communication ones in this paper.

Ross analysed transient responses of microwave networks [14]. A 0.2 ns pulse and a microwave step modulated source are used in the experiment. Furthermore, Ross described transient behaviour of antennas [15] and took out the first UWB communications patent [16]. The patent claims "an electromagnetic signal communication system utilising short baseband pulse signals of sub-nanosecond duration employs dispersionless, broad band antenna transmission line elements for generating and preserving the character of the short base-band pulses in respective transmitter and receiver sub-systems". That is nothing less than impulse radio of nowadays.

Another pioneer Harmuth proposed to use Walsh functions instead of sine-cosine functions in transmissions of information and analysed in detail [17–20, 25]. Ref. [18] is the first book in UWB technology. Though both Walsh and sine-cosine functions are orthogonal functions, Walsh functions are two-valued functions and consisted of rectangular waves. The selective reception of signals in mobile communications and a correlation receiver are shown in ref. [19,26,27]. Antenna radiation characteristics when non-sinusoidal electromagnetic waves are driven and propagation characteristics of that were also analysed by Harmuth [18–24]. From the description above, one could express that Harmuth's results are connected to code division multiple access (CDMA) in nowadays.

Chapter 3

Analysis of Baseband Signals

There are two systems in the representation of wireless signal. One is the pass-band system which describe wireless signals actually and the other is the equivalent low-pass system which describe wireless signals as a low-pass system with no carrier-frequency. In general, the signal expression in wireless transmissions is given as the equivalent low-pass system which is described using complex number. A fractional bandwidth of wireless systems is typically less than 5 %, and our interest is information component, which rides in carrier wave, not the behaviour of sinusoidal carrier wave itself. Therefore, it is not efficient to analyse a signal including carrier wave which need a so wide frequency range. As the result, we can state that the analysis in the equivalent low-pass system is efficient because of reducing the amount of computer operations.

However, we can not treat the WBT signal in the equivalent low-pass system, because WBT signal has not a sinusoidal carrier wave. It is required for WBT to make an analysis method which is based on real signal analysis.

3.1 Transmission Theory of a Real Signal

We mention how to treat real signals in time and frequency-domain. We regard the system of considering as a linear time-invariant (LTI) system.

3.1.1 Time Domain Representation

The relationship between a transmitting and receiving signal in a LTI system is

$$
\begin{aligned}
r(t) &= \int_{-\infty}^{\infty} h(t-\tau)s(\tau)d\tau + n(t) \\
&= h(t) \otimes s(t) + n(t),
\end{aligned}
\tag{3.1}
$$

where $r(t)$ is a receiving signal, $h(t)$ is a impulse response of a LTI system, $s(\tau)$ is a transmitting signal, $n(t)$ is a additive noise, τ is delay, and $\otimes$ denotes convolution integral. These variables are belong to real numbers.

3.1.2 Frequency Domain Representation

We consider the LTI system same as 3.1.1 in frequency-domain. The relationship is

$$
\begin{aligned}
R(f) &= H(f)S(f) + N(f) \\
&= \{H^{+}(f)S^{+}(f) + N^{+}(f)\} \\
&+ \{H^{-}(f)S^{-}(f) + N^{-}(f)\},
\end{aligned}
\tag{3.2}
$$

where $R(f)$, $H(f)$, $S(f)$, and $N(f)$ are the Fourier transforming of $r(t)$, $h(t)$, $h(t)$, and $n(t)$. The subscripts of $+$ and $-$ denote positive frequencies and negative frequencies, respectively. We must consider positive and negative frequencies when we treat the Fourier transform of real signals.

3.1.3 Real Signal and Analytic Signal

We regard $r(t)$, $s(t)$ and $n(t)$ as $x(t)$, and $R(f)$, $S(f)$, and $N(f)$ as $X(f)$. We assume that $x(t)$ denotes a real signal, and the analytic signal of $x(t)$ is $a(t)$. Although we need not the restrict ($x(t)$ is a real signal) in general, we treat $x(t)$ as a real signal in this paper. The analytic signal $a(t)$ is a complex signal which consists of doubling the positive spectrum part of the original signal $x(t)$. Therefore, $a(t)$ is defined as follows:

$$a(t) = 2\int_0^{\infty} X(f)e^{j2\pi ft}df = x(t) + j\hat{x}(t), \tag{3.3}$$

and

$$\mathrm{Re}\,[a(t)] = x(t), \tag{3.4}$$

where the coefficient 2 in the first term of the right part of Eq.3.3 is for the satisfaction of Eq.3.4, and the symbol $\hat{}$ in the second term of the right part of Eq.3.3 denotes Hilbert transform. The symbol $\mathrm{Re}\,[\ ]$ in Eq.3.4 denotes that we take the real part of the complex number. Real signals have the relationship of complex conjugate between $X^{+}(f)$ and $X^{-}(f)$. Assuming that we have only $X^{+}(f)$, we can calculate $X^{-}(f)$ in real signals. e.g., the channel characteristic data taken by VNA (vector network analyser) are equivalent to $X^{+}(f)$, therefore, we need to add $X^{-}(f)$ component after the measurement.

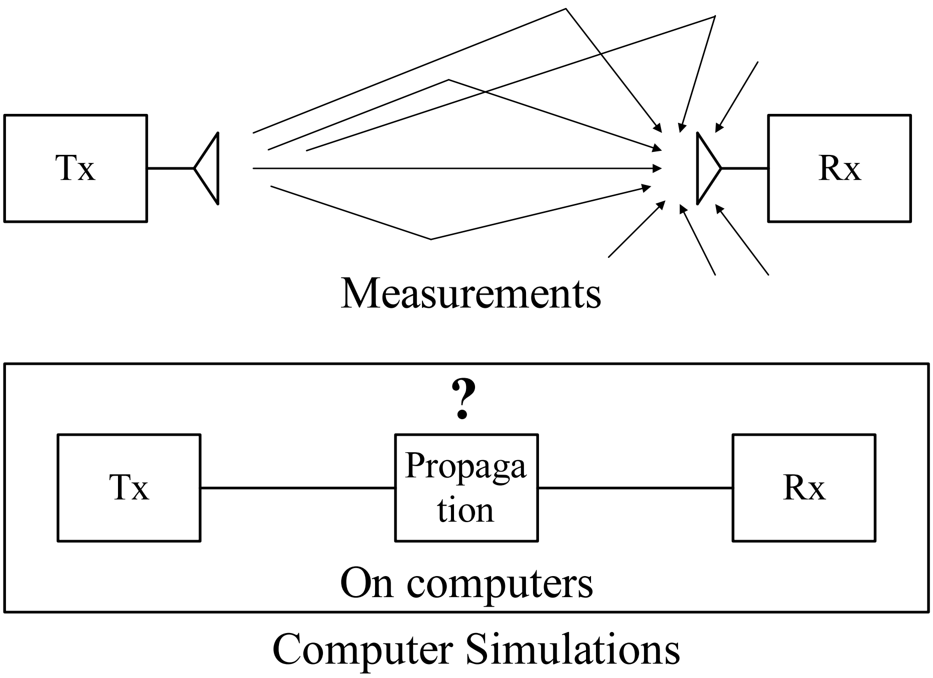

Fig. 3.1 Measurements and computer simulations

3.2 BER Calculation Method

3.2.1 Measurements and Simulation on Computers

There are two method to evaluate transmission characteristics in terms of BER. One is a measurement using a WBT transmitter and receiver, and the other is a computer simulation. It is not easy to construct a WBT transmitter and receiver for the sake of measuring BER. Computer simulation is easier than measurement. However, the problem is how to treat the propagation factor of WBT as shown in Fig. 3.1. We try to resolve the above problems using the fusion of measurement and computer simulation: i.e., we obtain only channel characteristic data using VNA, and other parts are operated on computers.

3.2.2 Operation Method

The operation method of BER calculation is shown in Fig. 3.2. The different point from conventional wireless system simulation is that we must deal with time-domain signals as real numbers. We explain Fig. 3.2 as follows:

Signal Generation

Data stream, which is transmitting signal, is generated on computers. We adopt Manchester encoding scheme to data stream in this paper. Manchester encoding contains information as a transition of voltage not voltage itself. We set the logic as voltage transition is High (Low) to Low (High) then logic '1' ('0'). Note that this definition is the same as the original reference of Manchester encoding, however, an opposite definition for IEEE802.4 etc. [12]. The number of bits contained in one data stream is arbitrary; we choose 200-bit in this paper because of sampling points.

Multiply Data Stream by Channel Characteristics

We transform data stream to frequency-domain by FFT (fast Fourier transform), and multiply it by channel characteristics which is taken by VNA. We add complex conjugate for the channel characteristics data in the event of this.

BER Calculation

We transform the data stream which multiplied by channel characteristics to time-domain by IFFT (inverse fast Fourier transform), and this becomes receiving data. We also calculate the power of receiving data to calculate BER curve; i.e., E_b/N_0

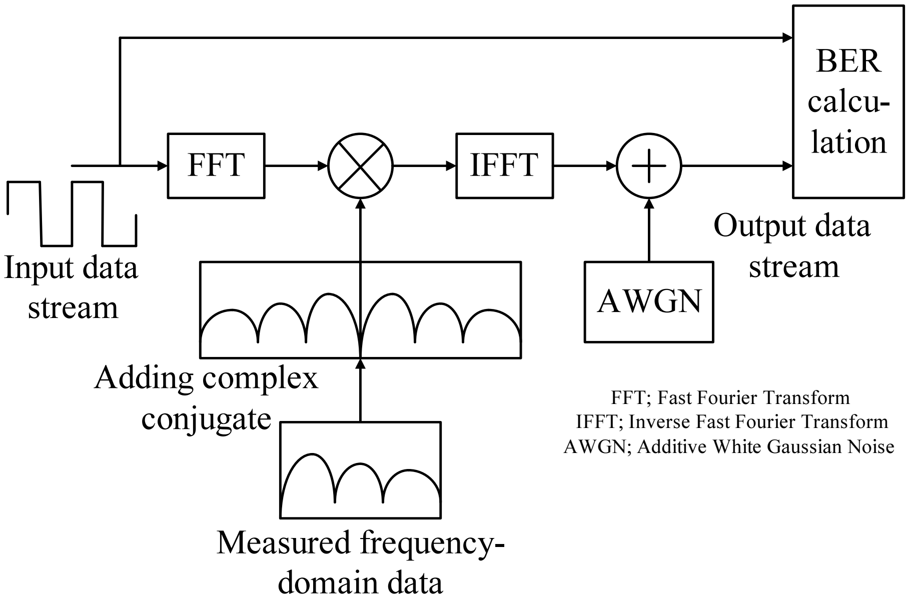

Fig. 3.2 Procedure of BER calculation (A block-by-block processing)

vs. BER. The BER can be calculated from comparing transmitting data with receiving data which is regarded to synchronise ideally. In the event of this, we add AWGN (additive white Gaussian noise). We repeat the above process at 10^4, and can calculate to one pair of E_b/N_0 vs. BER. Therefore, we repeat it until BER curve is described.

3.3 Validity of the Analysis Method

3.3.1 Identification Between Time and Frequency Domain Measurements

Our method of BER calculations is not use BER testers nor oscilloscopes. These equipment makes time-domain measurements possible and is used generally in BER measurements of conventional wireless systems. Furthermore, our method is different from a full computer simulation in time-domain which is used generally in the evaluation of conventional wireless systems too. The following is required to guarantee the validity of our method: The received waveform made from transmitting signal generated on computers and frequency-domain channel characteristics taken by a VNA conforms to the received waveform measured directly by a oscilloscope.

Fig. 3.3 shows an example of the validity. Fig. 3.3(a) indicates a transmitting signal which is generated by a data generator. The information bits indicate {1 0 0 0 1 0 0 1 1 0 1 0 1 1 1} because we adopt Manchester encoding. The solid line in Fig. 3.3(b) indicates a receiving signal which is measured by a digital storage oscilloscope (DSO). The dotted line in Fig. 3.3(b) is a calculated waveform on a computer using a channel characteristic taken by a VNA. We use a pair of discone antenna which operate over 100 MHz because our DSO can operate for 500 MHz bandwidth and we need to measure directly using the DSO. When we compare the two waveforms which is shown Fig. 3.3(b), we find that almost the same waveforms are obtained. Therefore, we can use the method calculating on a computer using a channel characteristic taken by a VNA instead of direct measurements using a DSO. We call this method as *VNA-PC method* hereafter.

3.3.2 Generation of Multipath Received Waveform Using Measured Channel Characteristics

We consider making multipath environments in a radio anechoic chamber. A certain multipath environment can be made easily setting up reflection boards in the

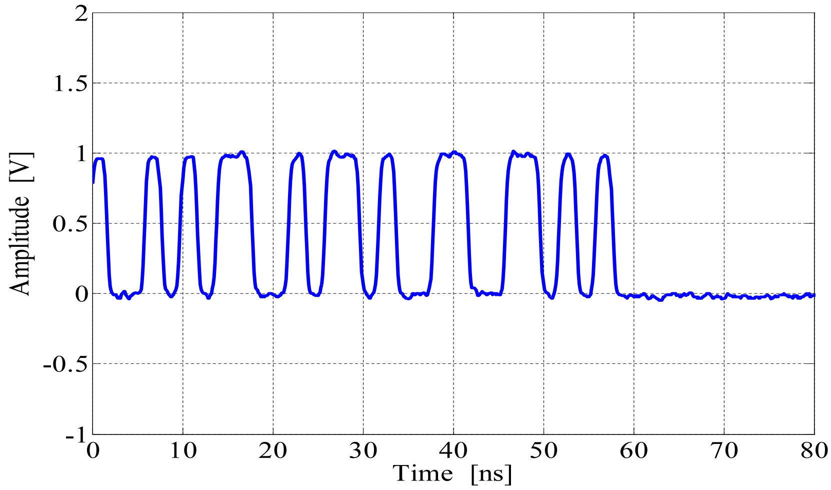

(a) Tx signal

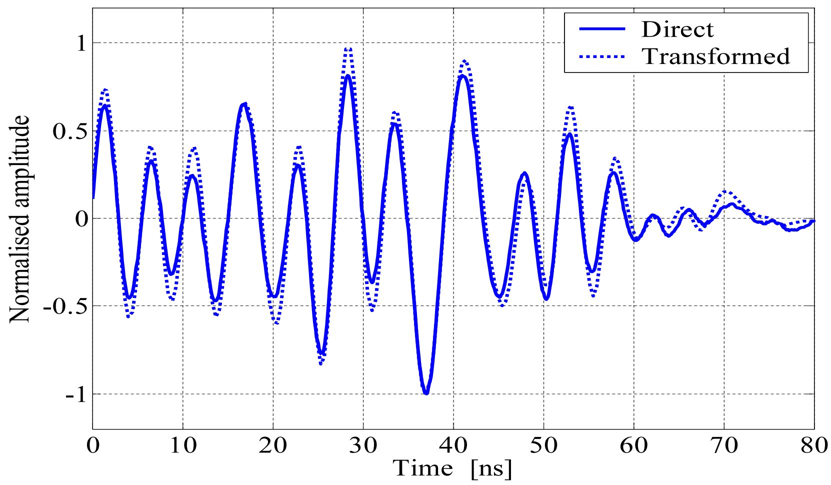

(b) Rx signal

Fig. 3.3 Direct and transformed waveform radio anechoic chamber. However, the combination that how many reflection boards and where to set up is infinite. Even though we limit the combination of reflection boards, time cost is still less effective. We worked out, therefore, the way to generate arbitrary multipath environments. The method is as follows: First, we take the channel characteristic of free space (no reflection boards) in a radio anechoic chamber. Second, we multiply the channel characteristic by a transmitting data which is transformed to frequency-domain using FFT on a computer. This operation generates a receiving data in free space. Third, we add the receiving data (direct wave) and reflection waves which are made by delaying the direct wave and decreasing that's amplitude taking light speed, reflection coefficient, and propagation loss into consideration.

Fig. 3.4 indicates the validity of this method. Fig. 3.4(a) shows a transmitting signals and the data bits is {1 0 0 0 1 0 0 1 1 0 1 0 1 1 1} because we adopt Manchester encoding. Fig. 3.4(b) indicates a received waveform in free space and this waveform is generated from on a computer using the VNA-PC method. Fig. 3.4(c) gives the almost same waveforms, where the solid and dotted lines indicate received waveforms in a real measurement environment and a virtual environment on a computer, respectively. We assume an environment in which one reflection board is set up. When we assume that the waveform in Fig. 3.4(b) and the dotted line in Fig. 3.4(c) are $x(t)$ and $y(t)$, $y(t)$ is made on a computer;

$$y(t) = x(t) - 0.45x(t - \tau), \tag{3.5}$$

where the negative sign of the right hand of Eq.3.5 is caused by our assumption that reflection coefficient is -1, the coefficient 0.45 is a propagation loss. We set τ of Eq.3.5 as 4.5 ns. We can state the validity of this method from Fig. 3.4.

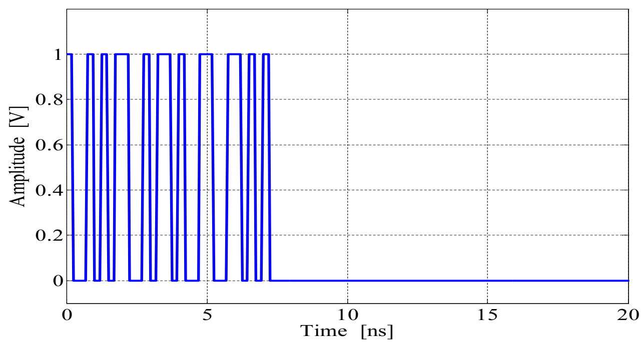

(a) Transmitted waveform

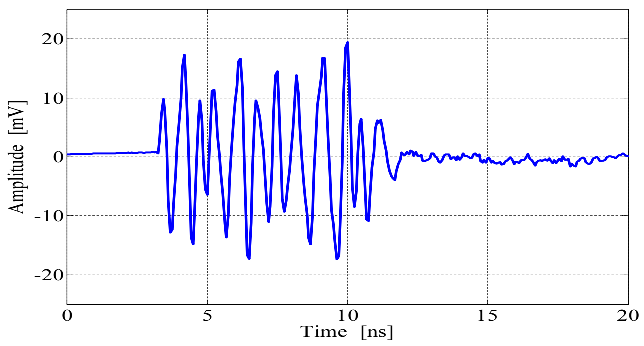

(b) Received waveform (Free space)

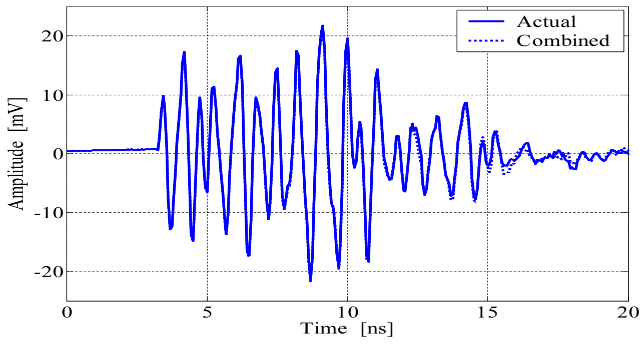

(c) Received waveform (Multipath, pass difference $\Delta d = 1.2$ m)

Fig. 3.4 Received waveforms; one reflection board is set up actually (solid line) vs. Combined waveform on computers (dotted line)

Chapter 4

Experiments under Free Space in Time and Frequency Domain

We describe WBT experiments. We use Manchester, RZ and NRZ codes as line signal codings in the experiments. One might consider to know the transmission characteristics for a single pulse itself (not sequence). We had also carried out transmission experiments using single pulse. The results are given in the appendix A.

4.1 Equipment

Equipment used in the experiments are listed as follows:

- data generator (DG) Tektronix DG2040 (Fig. 4.1(a))
- digital storage oscilloscope (DSO) Tektronix TDS714L (Fig. 4.1(b))
- vector network analyser (VNA) ADVANTEST R3767CG (Fig. 4.1(d))

The main specifications are also shown in Table 4.1.

(a) DG2040

(b) TDS714L

(c) R3767CG

Fig. 4.1 Equipment used in the measurements

Table 4.1 Main specifications

DG clock	500 MHz (pulse width is 2 ns)
DG amplitude	1 V
DSO bandwidth	500 MHz
DSO vertical resolution	8-bit (S/N 50dB)
Sampling method	Equivalent timing sampling at 10 GS/s
VNA frequency range	300 kHz–8 GHz (available)
Antenna type	Discone
Antenna height	2 m
Antenna distance	5 m

4.2 Data Encoding Scheme

We chose Manchester, RZ, and NRZ encoded signals for our experiments because this is the first study on WBT and we would like to investigate its basic performances. These encoding schemes are very basic in the field of data transmission, which matches our requirements. Although we do not consider RZ or NRZ to be suitable for WBT, we use these two encoding schemes for the purpose of comparison with Manchester encoding. The main advantages of using Manchester encoding, compared to RZ or NRZ encoding, are as follows:

- It is possible to prevent the generation of lower frequency components when successive identical codes, such as '11111', are transmitted.
- It is easy to perform clock recovery.

On the other hand, Manchester encoding also has a disadvantage:

- The required bandwidth is twice that of NRZ.

Manchester encoding is invented in the University of Manchester as the name suggests.

4.3 Setup

A schematic diagram of the experimental setup is shown in Fig. 4.2. All experiments were carried out in a radio anechoic chamber.

A data generator (DG) is used as a transmitter and a digital storage oscilloscope (DSO) is used as a receiver. A pair of discone antennas [28] is used at the transmitter and receiver sides because, due to its simple structure, a discone antenna is considered to have a flat amplitude spectrum and a linear phase characteristic over a given band. The antenna is one of the most important devices for wide-band systems [29–32]. The antenna shown in Fig. 4.3 is used in our experiments. This antenna is a discone antenna consisting of 12 aluminium pipes. Although a discone antenna generally consists of a disc and a cone, as the name suggests, for the present study, we designed and constructed a discone antenna using aluminium pipes. Fairly large sized antennas, $(1\text{m})^3$, were required in order to observe received waveforms directly with the 500 MHz DSO. We designed the discone to operate at over 100 MHz. Acquisition of data is performed by connecting the DSO to a personal computer (PC). A vector network analyser (VNA) is used to obtain frequency-domain data, such as voltage standing wave ratio (VSWR) and transmission characteristics between the transmitting and the receiving antennas, i.e., S_{21}, assuming that the index of the transmitting antenna is '1', and that of the receiving antenna is '2'. Figure 4.4 shows the VSWR characteristic of the discone antenna. The VSWR is suppressed below 2 at the frequency range from 100 MHz to 600 MHz (fractional bandwidth: 1.4[1]).

4.4 Method

On the transmitter side, Manchester, RZ, and NRZ encoded signals are generated from the DG and are supplied to the transmitting antenna directly. We generate a 15-bit code pattern signal {1 0 0 0 1 0 0 1 1 0 1 0 1 1 1} using the DG and adopt

[1] Defined in 6.1.2.

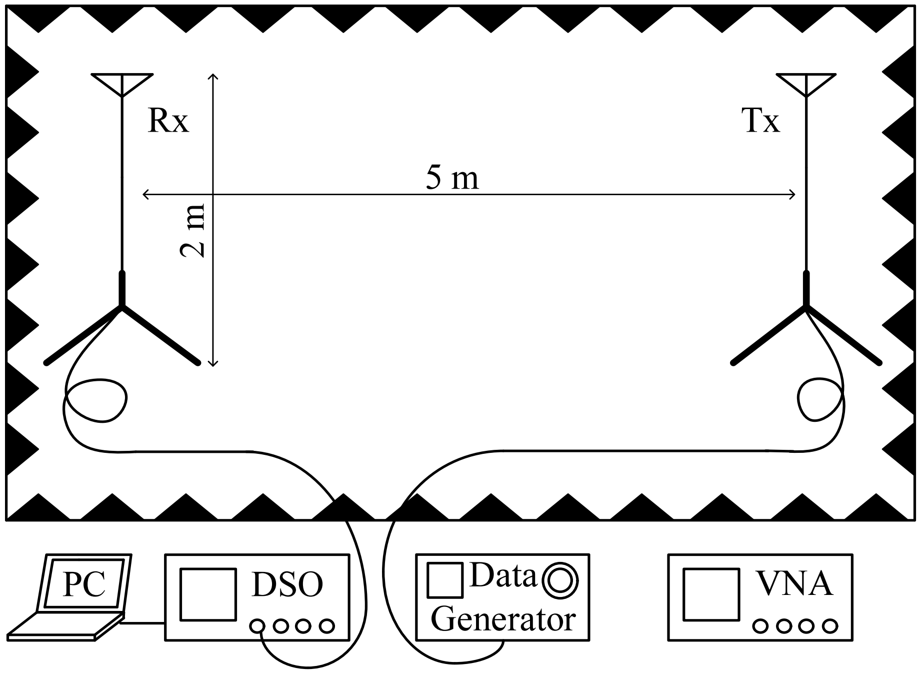

Fig. 4.2 Experimental setup

positive logic. Because the amplitude of generated signals from DG is +1V, as shown in Table 4.1, logic ‘1’ (‘0’) corresponds to +1 (0)V, in accordance with the rule.

On the receiver side, the amplitude of a received waveform is measured with the DSO. Considering the DSO bandwidth and the designed discone antennas, the clock of a generated waveform (Manchester, RZ, or NRZ) from the DG is chosen as 500 MHz (pulse width: 2 ns). The height from the ground to the feed point of the antenna is 2 m, and the distance between the transmitting and receiving antennas is 5 m, as shown in Fig. 4.2.

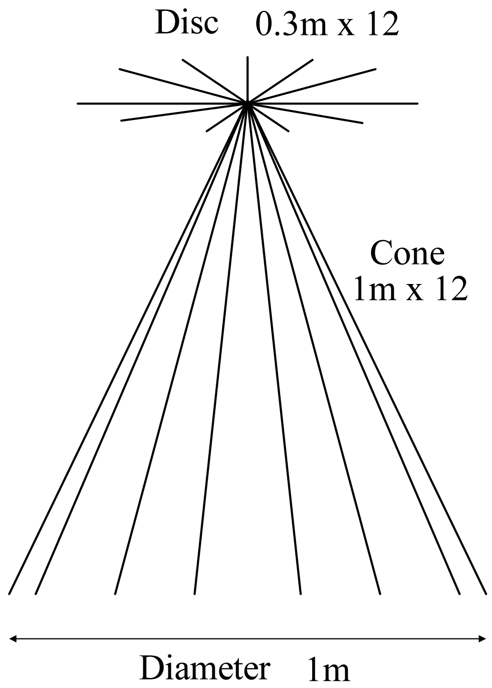

(a) Size

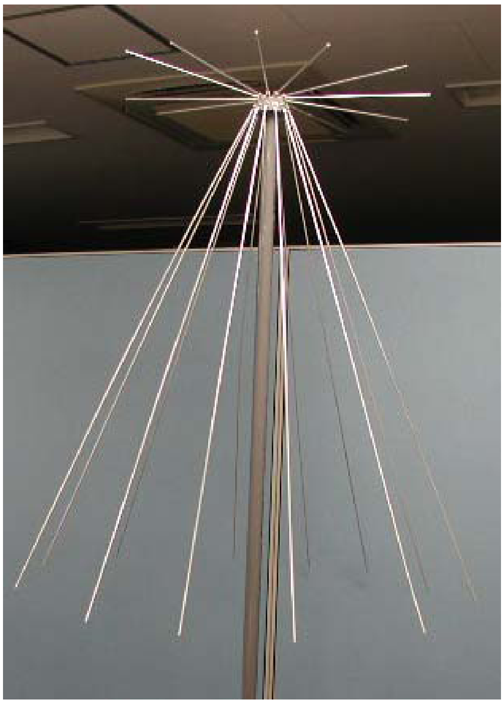

(b) View

Fig. 4.3 Designed discone antenna

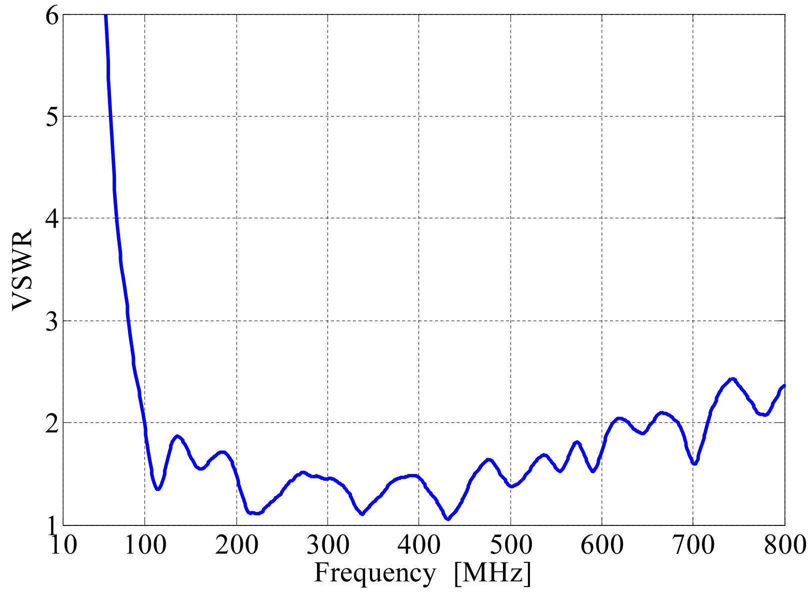

Fig. 4.4 VSWR characteristic of the discone antenna

4.5 Results

4.5.1 Channel Characteristics

A measured channel characteristic (S_{21}) in the frequency-domain is shown in Fig. 4.5. In Fig. 4.5(a), a −6 dB/octave line, which will be described in 6.1, is depicted. We consider that the ripples shown in Fig. 4.5(a) are the results of reflected waves from a part of the floor in which there is no electromagnetic absorbers. In addition, we find that an almost linear phase characteristic is obtained, as shown in Fig. 4.5(b).

Data Transmission Experiments

The DG output and received waveforms of the Manchester, RZ, and NRZ encodings are shown in Fig. 4.6 – Fig. 4.8. In Manchester encoding, we set the logic

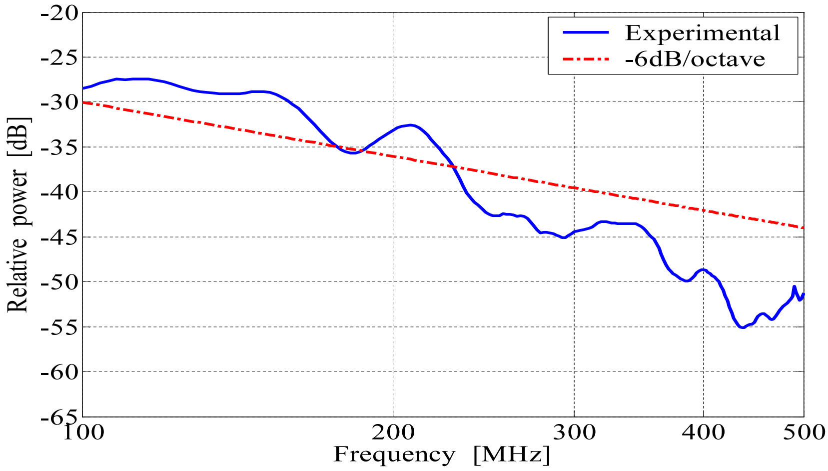

(a) Relative power (horizontal axis is logarithm scale.)

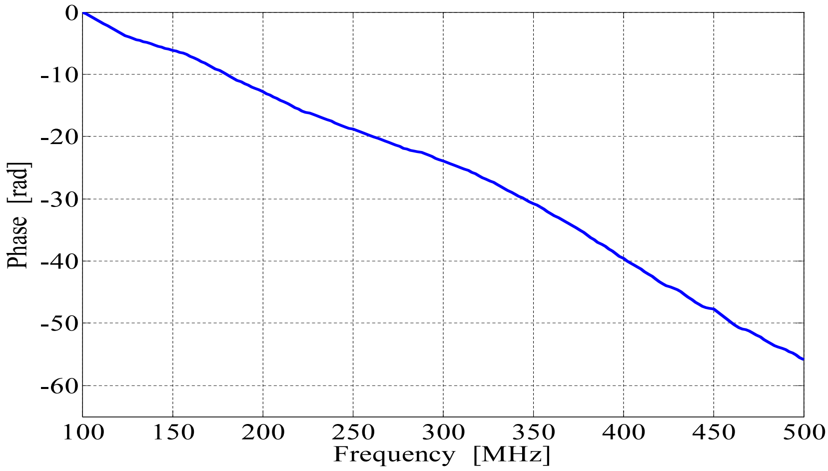

(b) Phase

Fig. 4.5 Measured transmission characteristics in the frequency-domain (S_{21})

such that voltage transition is High (Low) to Low (High), then logic ‘1’ (‘0’). Note that this definition is the same as the original reference of Manchester encoding, although opposite to the definition given in IEEE802.4 [12]. In RZ and NRZ encoding, we adopted positive logic, as described in 4.4. The data detection results are also shown in Fig. 4.6(c) – Fig. 4.8(c). Here, the letter ‘x’ indicates the occurrence of an error. In Manchester encoding, the data that could be detected correctly are shown in Fig. 4.6(c). In RZ and NRZ encoding, we set the threshold voltage to 0 V. We can find one error in RZ and two errors in NRZ, as shown in Fig. 4.7(c) and Fig. 4.8(c), respectively. Figure 4.6 indicates a 250 mega-bits per second (Mbps) WBT using Manchester encoding, because the pulse width is 2 ns. Note that Manchester encoding halves the data rate compared to NRZ on the same pulse width, as mentioned in 4.2.

Comparing these three encoding schemes, we can state that only Manchester encoding is detected correctly, as shown in Fig 4.6(c). We will calculate the bit error rate (BER) for Manchester, RZ, and NRZ encoding in the next section.

BER Calculations

We calculate the BER for the three (Manchester, RZ, and NRZ) encoding schemes for the purpose of confirming the above hypothesis. We measured the transmission characteristics in the frequency-domain using a VNA, as shown in Fig. 4.5 and calculated the BER using a PC. The procedure is shown in Fig. 3.2. We generated a 240-bit data stream with 4,806 samples per trial. We repeated this procedure 10^5 times. The frequency-domain method using a VNA and a PC (VNA-PC

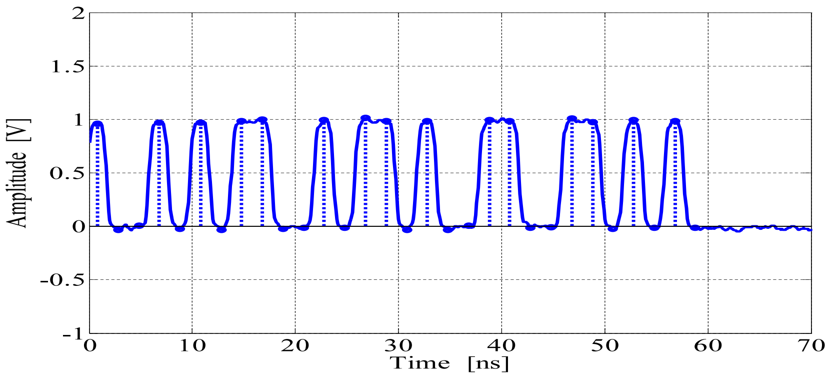

(a) Generated Manchester waveform (DG output)

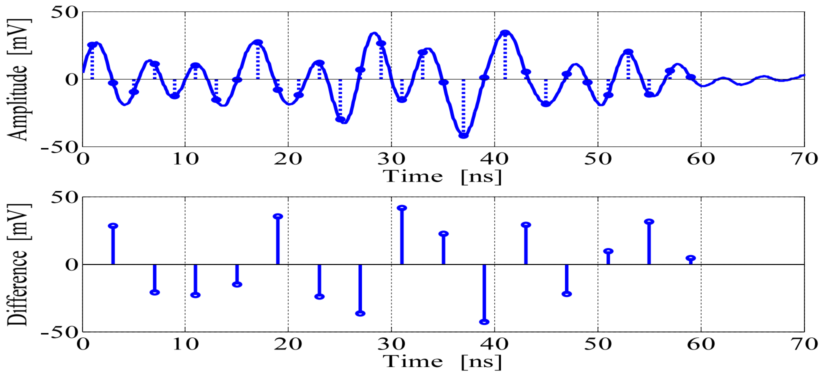

(b) Received waveform

Tx data	1	0	0	0	1	0	0	1
Rx data	1	0	0	0	1	0	0	1
Tx data (cont.)	1	0	1	0	1	1	1	
Rx data (cont.)	1	0	1	0	1	1	1	

(c) Detection result

Fig. 4.6 Measured transmission characteristic of Manchester encoding

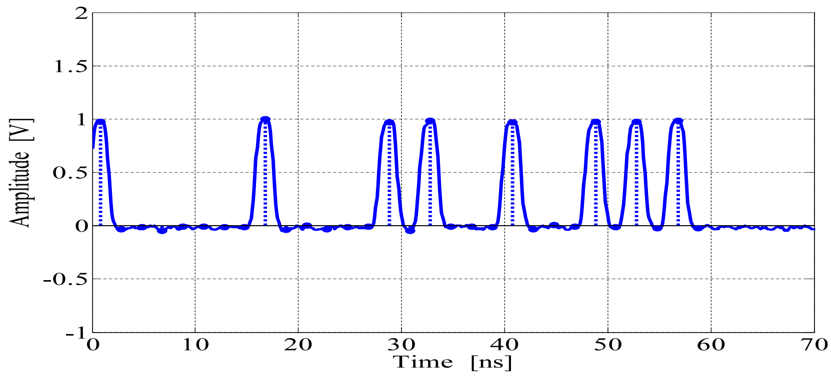

(a) Generated RZ waveform (DG output)

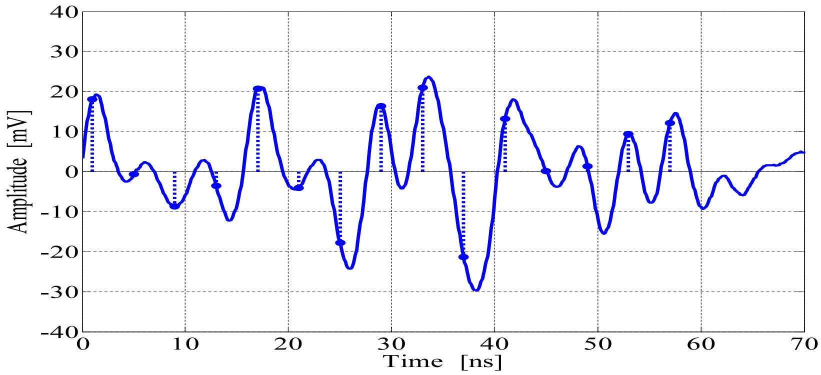

(b) Received waveform

Tx data	1	0	0	0	1	0	0	1
Rx data	1	0	0	0	1	0	0	1
Tx data (cont.)	1	0	1	0	1	1	1	
Rx data (cont.)	1	0	1	x	1	1	1	

(c) Detection result

Fig. 4.7 Measured transmission characteristic of RZ encoding

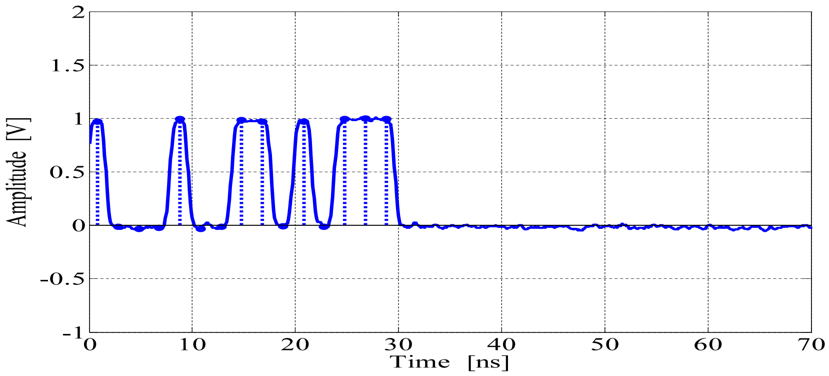

(a) Generated NRZ waveform (DG output)

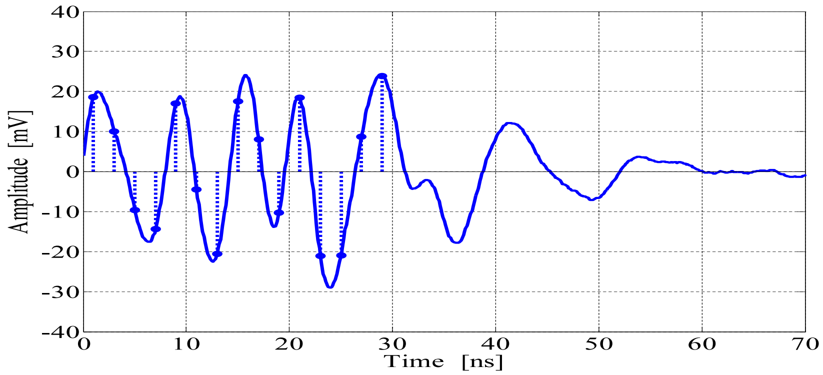

(b) Received waveform

Tx data	1	0	0	0	1	0	0	1
Rx data	1	x	0	0	1	0	0	1
Tx data (cont.)	1	0	1	0	1	1	1	
Rx data (cont.)	1	0	1	0	x	1	1	

(c) Detection result

Fig. 4.8 Measured transmission characteristic of NRZ encoding method) was adopted considering the number of data bits needed in BER calculations. We need at least 10^7 bits to calculate BER until 10^{-6}. Our DSO has 250 K of memory and must operate at 10 GS/s (as shown in Table 4.1). This means that the maximum recording time is 25μs, i.e., 6,250-bit per measurement, using Manchester encoding. Measurement must be conducted 1,600 times per encoding scheme because our DSO and DG are not controlled automatically. This is not so efficient. Therefore, we adopted the VNA-PC method shown in Fig. 3.2. Figure 4.9 indicates the time-domain output waveforms calculated from the measured frequency-domain data. The input data is {1 0 0 0 1 0 0 1 1 0 1 0 1 1 1}, which is the same code pattern used in the experiment. Comparing Fig. 4.6(b), Fig. 4.7(b), and Fig. 4.8(b) with Fig. 4.9, reveals that almost the same waveforms are obtained. Therefore, we can evaluate the BER using the measured frequency-domain data. Figure 4.10 indicates the BER characteristics obtained using the measured frequency-domain data. When we compare the three encoding schemes shown in Fig. 4.10, we found that large error-floors in RZ and NRZ. These phenomena become dominant when successive identical code patterns are generated for a long time (such as {1 1 1 1 1} or {0 0 0 0 0}). In addition, we found that the BER for Manchester encoding is less than 10^{-3} for a S/N of over 20 dB. From the above results, we can conclude that Manchester encoding is suitable for WBT.

Summary

Although we carried out the experiment at a lower transmission data rate, namely 250 Mbps, using a large antenna because of the performance limit of the measure-

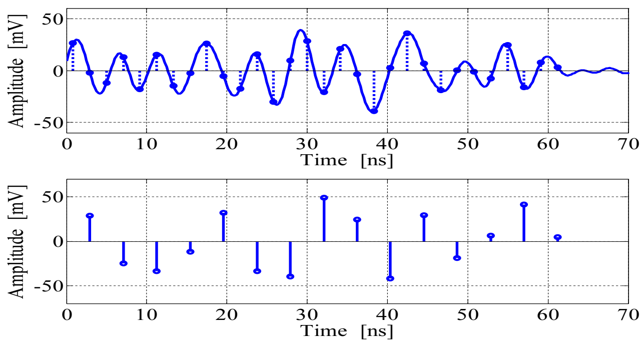

(a) Manchester

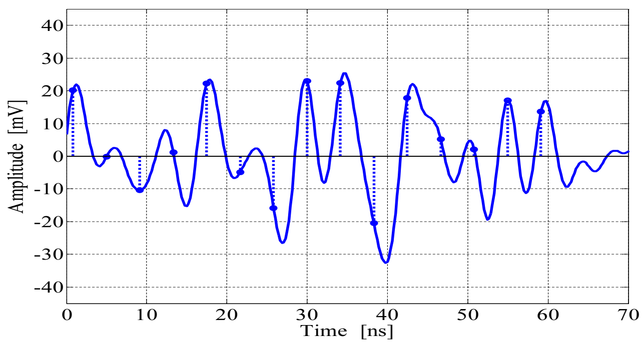

(b) RZ

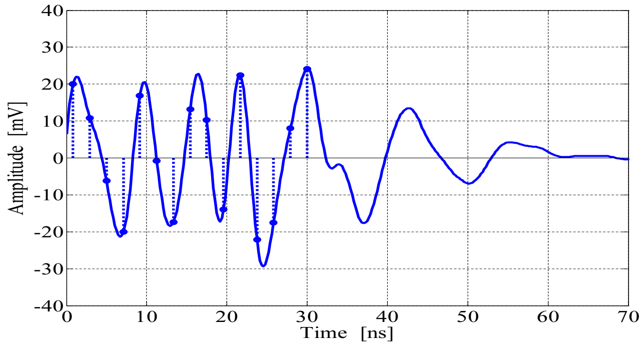

(c) NRZ

Fig. 4.9 Time-domain waveforms calculated from the measured frequency-domain data.

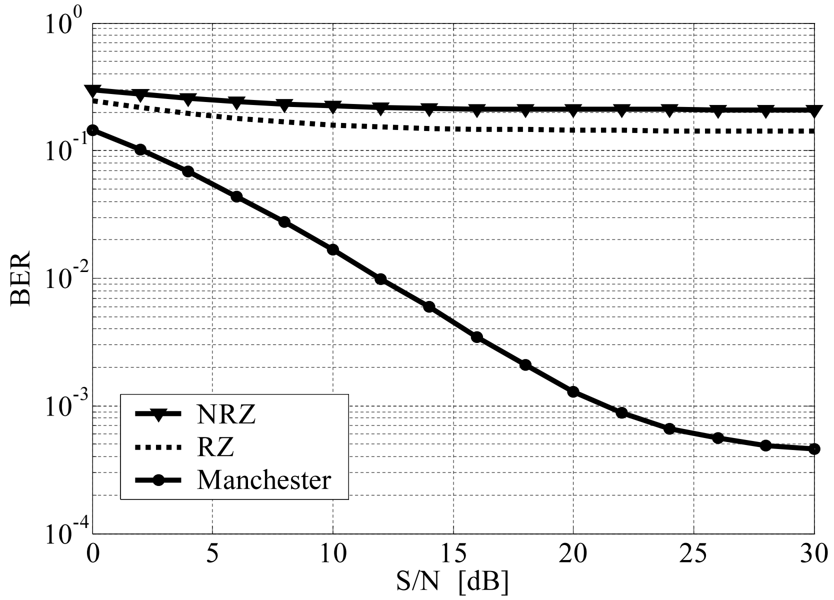

Fig. 4.10 BER characteristic using the measured frequency-domain data

ment equipment in the operational frequency range, the principle of the wireless baseband transmission was verified. We need to examine the parameters between the antenna bandwidth and the pulse width for the purpose of designing WBT systems. We will discuss that point in Chapter6.

Chapter 5

Experiments in Multipath Environments in Frequency Domain

VNA-PC method can perform instead of measuring in the time-domain using a DG and DSO as mentioned in 4.5.1. This means that we can use even smaller antennas than in Chapter4 because a VNA can be measured in a wide frequency range (to higher frequencies) comparing a DSO. We use only a VNA and not use a DG and DSO in this chapter.

5.1 Measurements of Channel Characteristics

5.1.1 Antenna Characteristics

The antenna shown in Fig. 5.1 is used in the present experiments. This antenna is a discone antenna with $(100\ \text{mm})^3$ and we made it from a copper board. We designed the discone to operate at the frequency range from 1 GHz to 6 GHz taking the VNA frequency range (Table 4.1) and a experiment of ease into consideration. We call this antenna *1G-discone antenna* after this to distinguish it from the discone antenna in Chapter 4 which operate over 100 MHz. Figure 5.2 shows the

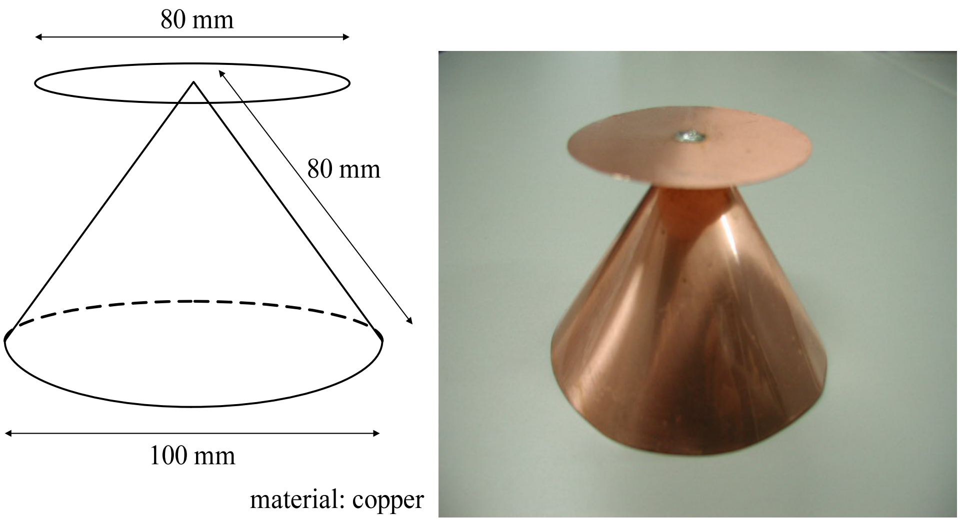

(a) Size (b) View

Fig. 5.1 Designed 1G-discone antenna

VSWR characteristic of the 1G-discone antenna. The VSWR is suppressed below 2 at the frequency range from 1 GHz to 6 GHz (fractional bandwidth: 1.4[1]).

5.1.2 Measurements using RF Network Analyser

There are two types in radio frequency (RF) network analysers. One is a scalar type and the other is a vector type. The vector type network analyser (VNA) is used in our experiments. Scattering (S) parameters can be taken by a VNA and S-parameters have complex numbers. Assuming that a Tx antenna is index '1' and a Rx one is '2', VSWR and channel characteristics are equal to $S_{11(22)}$ (reflection coefficients) and $S_{21(12)}$ (transmission coefficients), respectively. The number of measurement points is 801 in the frequency range from 300 kHz to 8 GHz (almost 10 MHz intervals). We carry out the 2-port full-calibration before measurements.

[1]Defined in 6.1.2.

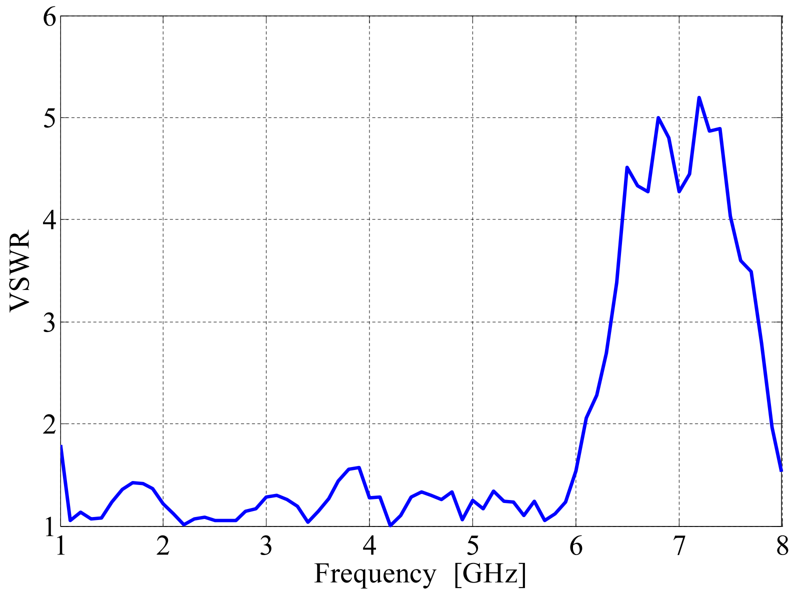

Fig. 5.2 VSWR characteristic of the 1G-discone antenna

5.1.3 Measurement Environments

A schematic diagram of the measurement environments is shown in Fig. 5.3. All experiments were carried out in a radio anechoic chamber the same in Chapter4. The reflection board shown in Fig. 5.3(b) is 1.8 m in length and 0.9 m in width which consisting of a foam polystyrene board and aluminium foil. We set up the reflection board vertically. The two experiments, (a) no reflection boards (Fig. 5.3(a) and (b) one reflection board (Fig. 5.3(b) were carried out. In Fig. 5.3(b), the difference of the two path Δd = 1.2 m; time difference $\Delta\tau$ = 4.0 ns. Antenna height is 1.5 m in both Tx and Rx.

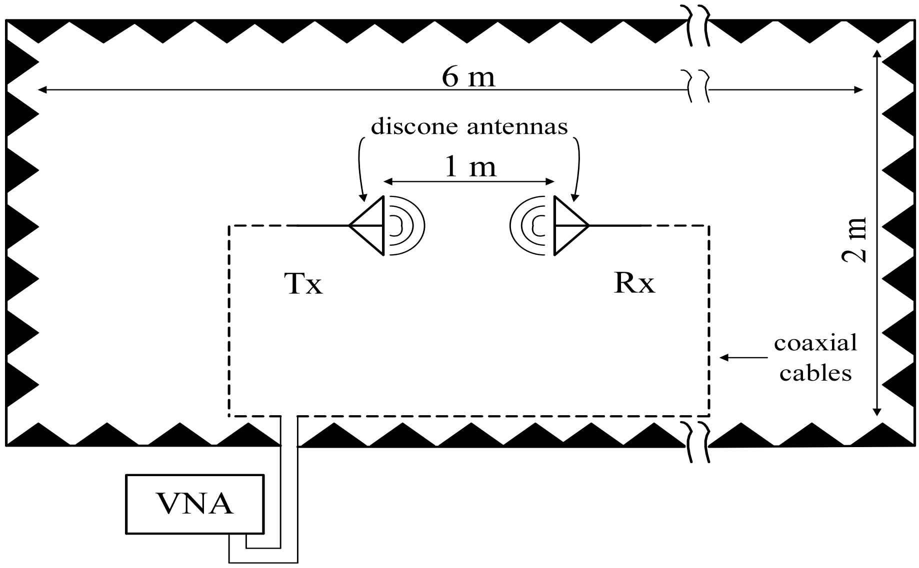

(a) No reflection boards

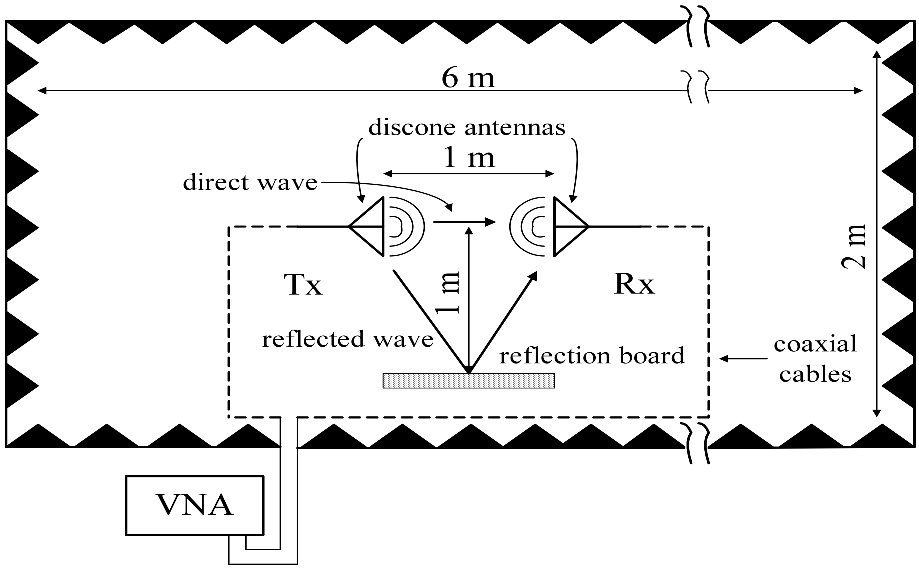

(b) One reflection board

Fig. 5.3 Measurement environments (upper view)

5.1.4 Channel Characteristics

Channel characteristics which are taken by the VNA are shown in Fig. 5.4. The showing frequency range of Fig. 5.4 is from 1 GHz to 6 GHz taking 5.1.1 into consideration. Figure 5.4(a) shows a characteristic of free space and the curve follows the −6 dB/octave characteristic which will be described in Chapter 6. The difference between the −6 dB/octave curve and the measured value near over 4 GHz shown in Fig. 5.4(a) is due to the vertical pattern disorder of the 1G-discone antenna. Figure 5.4(b) show a characteristics with a ripple due to a reflection board (phase interference). The frequency of the ripple is 250 MHz. This value follows the theory; i.e., $1/\Delta\tau = 1/4.0$ ns = 250MHz.

Another way to understand multipath characteristics is to observe the impulse response of a system. Figure 5.5 shows the impulse response of the environment shown in Fig. 5.3. This impulse response is calculated from the frequency domain (Fig. 5.4) using IFFT. An impulse occurs with 3.3 ns delay which is the propagation time between Tx antenna and Rx one. The response near 10–11 ns shown in Fig. 5.5(a) is due to multiple reflections between Tx antenna and Rx one which are caused by frequency components over the matching range. In Fig. 5.5(b), the response of the reflected wave is occurred with the 4 ns delay to the direct wave because $\Delta\tau$ is 4 ns as mentioned in 5.1.3.

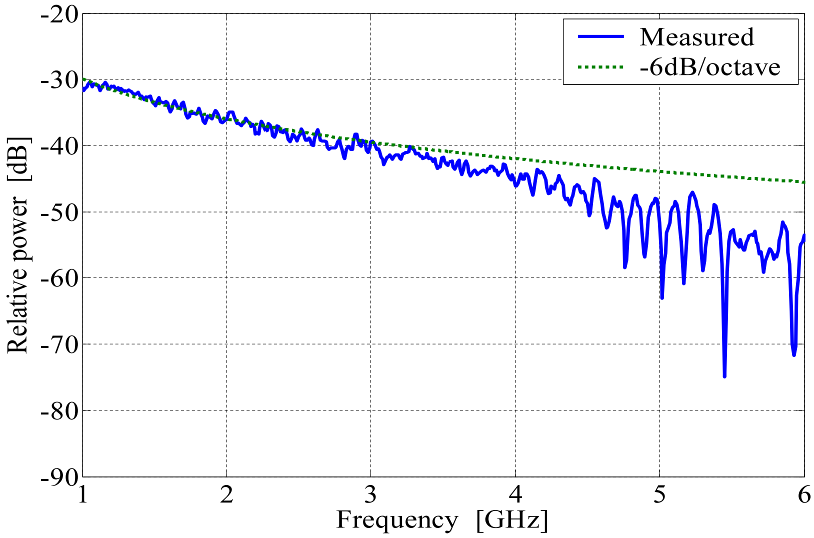

(a) No reflection boards

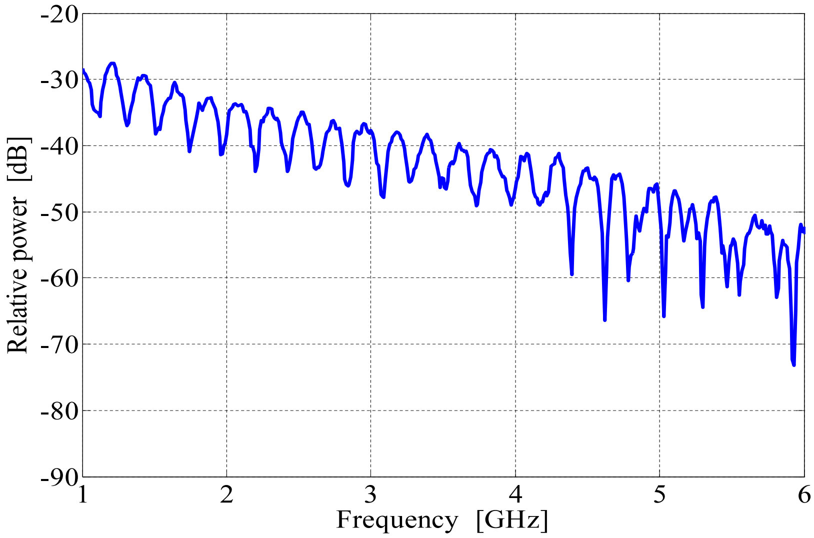

(b) One reflection board

Fig. 5.4 Channel characteristics

5.2 Evaluation of Channel Characteristics

5.2.1 BER Characteristics in the Environment

Figure 5.6 shows the BER characteristics in the measurement environment shown in Fig. 5.3. We treat the E_b/N_0 (the energy per bit to the noise spectral density ratio) to direct wave (not direct wave plus reflected wave) on the horizontal axis E_b/N_0 of Fig. 5.6. The two results are shown for a multipath environment. One is the measurement result in which set up the reflection board actually, and the other is the artificial multipath environment on a computer as mentioned in 3.3.2. The two results agree with each other as shown in Fig. 5.6. Therefore, we can state that arbitrary multipath environments can be generated on a computer using a channel characteristic for a direct wave. We adopt Manchester encoding scheme in this experiment, and the pulse width of the minimum unit is 2 ns taking the relationship between a pulse width and an antenna bandwidth which will be mentioned in 6.1.2 into consideration. The symbol length, therefore, is 4 ns because of Manchester encoding, and the data rate is 2.5 Gbps. Although error floor does not appear in free space, it appears in the multipath environment as shown in Fig. 5.6. The BER at that condition is 10^{-3} and this value is a limit of practical communications without equalisation or error collecting techniques. The number of delayed symbols is 10 because the reflected wave is arrived with the delay of 4.0 ns as mentioned in 5.1.3. Therefore, inter-symbol-interference (ISI) makes the error floor.

The performance curve of binary phase shift keying (BPSK) is also shown in

Fig. 5.6 to compare WBT with conventional wireless systems. The curve is the theoretical value for BPSK,

$$P_b = \frac{1}{2}\mathrm{erfc}\sqrt{E_b/N_0}, \tag{5.1}$$

where P_b is the bit error rate and erfc is the complementary error function. Almost 3 dB additional energy is required for WBT comparing with BPSK as shown in Fig. 5.6. However, a carrier around 250 GHz is needed to perform a 2.5 Gbps transmission by BPSK with the fractional bandwidth of 1 % (a typical value of conventional wireless systems). It is not easy to make such a 250 GHz transceiver and an antenna. Therefore, WBT is a candidate for high-speed wireless transmissions, e.g., A Gbps transmission using a GHz radio wave, although having a 3 dB-handicap to BPSK (in this paper).

5.2.2 BER Characteristics for the Variation of Reflection Coefficient

The BER characteristic for the variation of reflection coefficient γ is shown in Fig. 5.7. The number of delayed symbols is the same with 5.2.1; 10-symbol delay. The γ is changed at -1 (Multipath (Combined) in Fig. 5.6), -0.8, -0.5, -0.2, 0 (Free space in Fig. 5.6). We find that an error floor is appeared in $\gamma = -1$ and -0.8 near the BER of 10^{-3} to 10^{-4}. In other cases, practical WBT communications are realisable in multipath environments. Figure 5.7 tends to show better performances when γ is to be smaller.

5.2.3 BER Characteristics for the Direct Wave Power to Reflected Wave Power

Fig. 5.8 shows the BER characteristic for the received power of direct wave to that of reflected waves ratio with varying the number of delayed symbols. Assuming that the power of a direct wave is P_D and that of reflected waves (the sum total when above two waves are existing) is P_R, P_R/P_D is changed at -6 dB, -10 dB, -15 dB, and -20 dB. In Fig. 5.8(a), an error floor is appeared when P_R/P_D is -6 dB and -10 dB at the BER of 10^{-1} and 10^{-2}, respectively. Therefore, a practical communication is difficult when P_R/P_D is greater than -10 dB. In Fig. 5.8(b), an error floor is appeared when P_R/P_D is -6 dB only at the BER of 10^{-2} and a practical communication is realisable in the other values of P_R/P_D. In Fig. 5.8(c), the same tendency is shown in the case when the number of delayed symbols is 10. We summarise the result in this section such that a practical WBT communication is realisable in multipath environments when P_R/P_D is smaller than -15 dB.

5.2.4 BER Characteristics for Varying the Number of Paths

Although we have treated a 2-path model on the above sections, we change the number of reflected waves in this section. Figure 5.9(a) shows the BER characteristic of 3-path; direct wave plus two reflected waves. The number of delayed symbols is set to 15 taking Fig. 5.8(b) and Fig. 5.8(c) into consideration. The same result is obtained between Fig. 5.8(b) and Fig. 5.8(c) and the number of average delayed symbols is 15 at that condition. We set the received power of the second reflected wave equal to that of the first one. Fig. 5.9(a) gives a similar result to Fig. 5.8, and a WBT communication is realisable without equalisation or error collecting techniques when P_R/P_D is smaller than -15 dB. Figure 5.9(b) and Fig. 5.9(c) show the results of 4-path and 5-path, respectively. The number of delayed symbols is 10, 15, and 20 in 4-path and 5, 10, 15, 20, and 25 in 5-path, or the average is 15. Each reflected waves have equal power. Figure 5.9 shows that although the number of reflected waves is increased then the performance is decreased, the whole tends to depend on P_R/P_D. In particular, almost same values of BER are obtained for 3, 4, and 5 paths when P_R/P_D is -20 dB. Therefore, we can state that the dominant factor is the ratio P_R/P_D.

5.3 Discussions

The performance of WBT is inferior to that of BPSK with 3 dB at the BER of 10^{-4} in free space. Equalisation or error collecting techniques are required in the dense multipath environment such that P_R/P_D is greater than -10 dB. However, when the multipath environments P_R/P_D is smaller than -15 dB, a practical WBT communication is realisable without those techniques. The factor P_R/P_D is more dominant to BER characteristics than the number of paths, or P_R/P_D is a small value (e.g., -20 dB) then a WBT communication is realisable even there are many reflected waves, and vice versa.

A countermeasure for dense multipath environments ($P_R/P_D \geq -10$ dB), is to equalise channel characteristics as shown in Fig. 5.10(a). Fig. 5.10(b) shows the BER characteristics before equalisation and after equalisation. We equalise the frequency range from 700 MHz to 2 GHz.

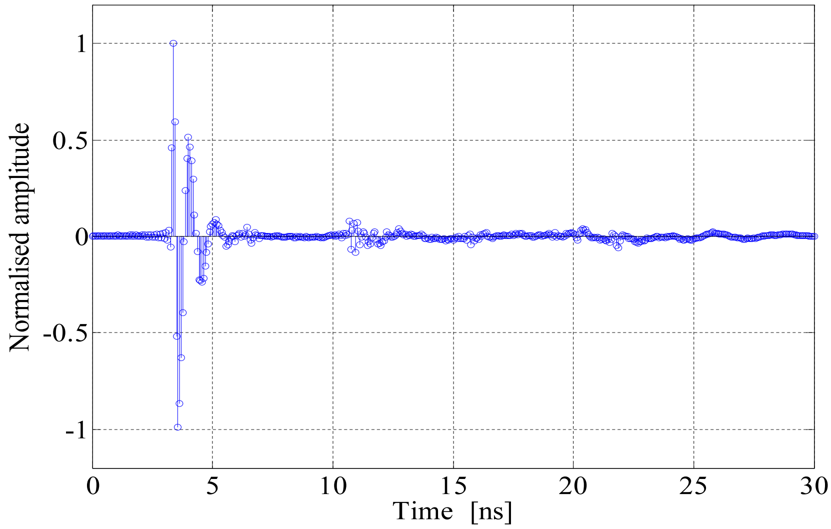

(a) No reflection boards

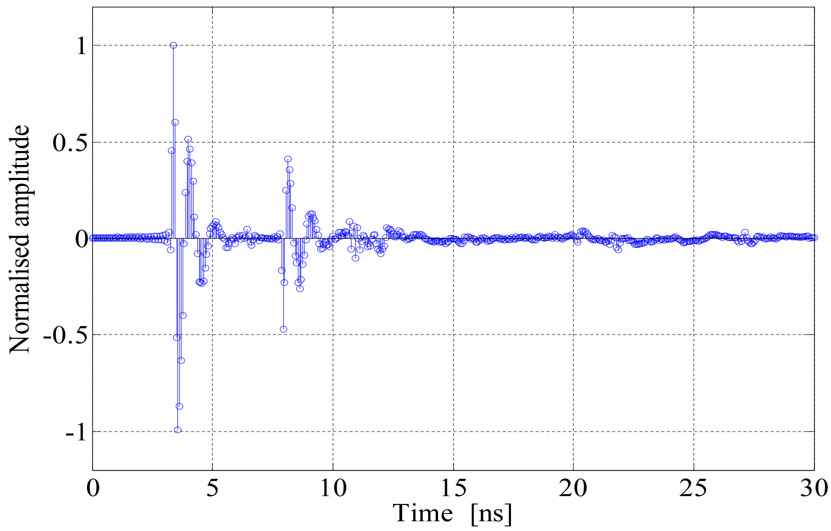

(b) One reflection board

Fig. 5.5 Channel impulse responses

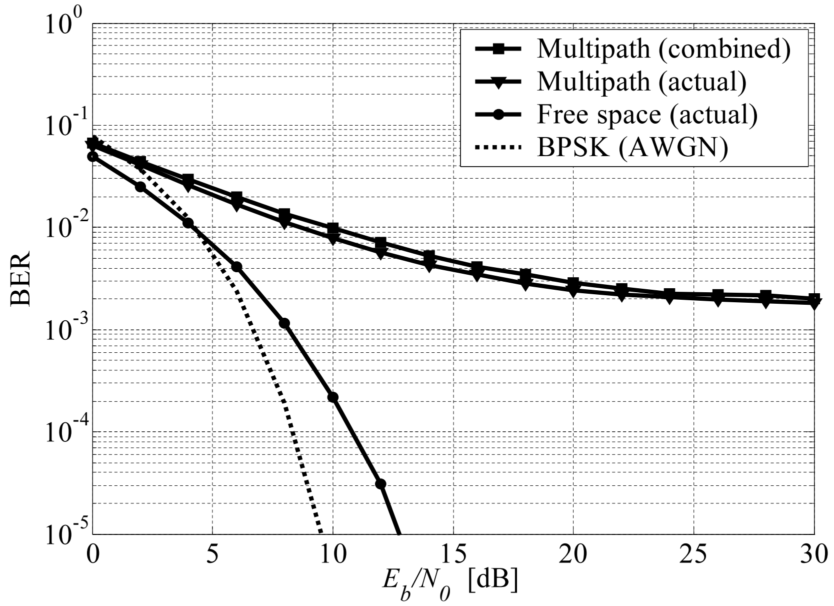

Fig. 5.6 BER characteristics in the measurement environment

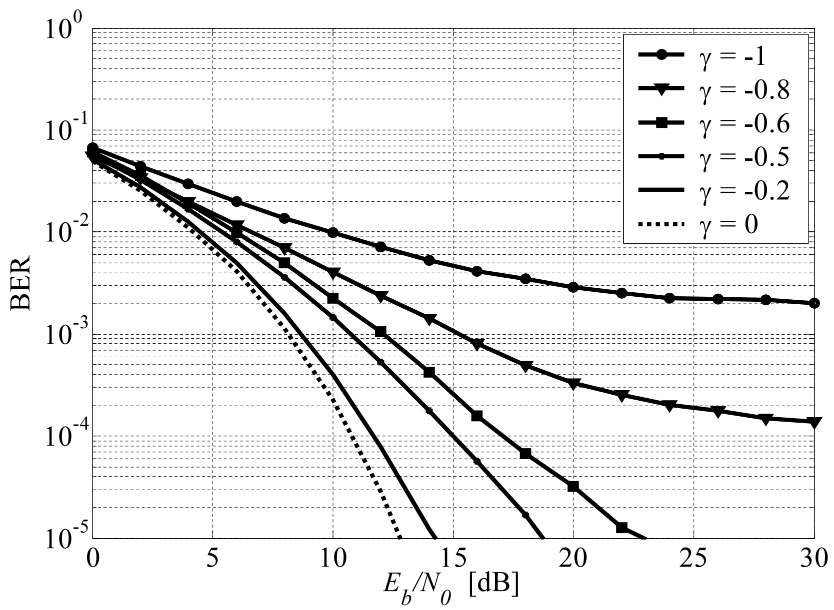

Fig. 5.7 BER characteristics with varying γ (reflection wave is arrived with 10-symbol delay of direct wave)

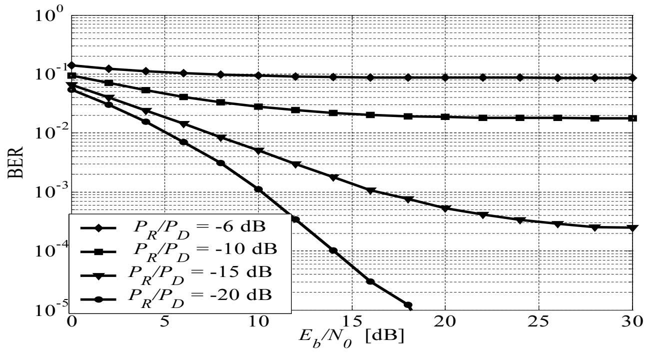

(a) 5-symbol delay

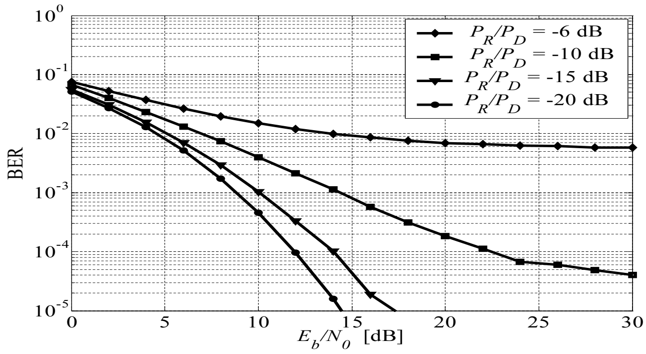

(b) 10-symbol delay

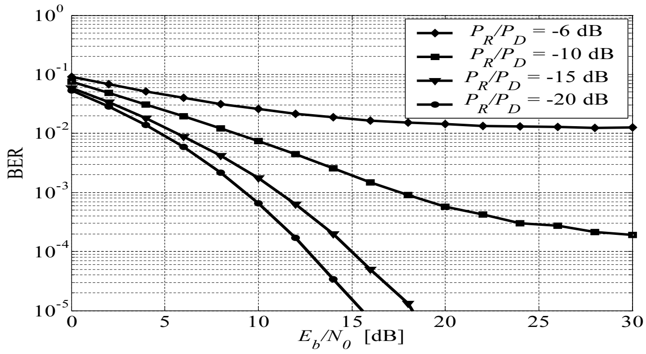

(c) 20-symbol delay

Fig. 5.8 BER characteristics with varying the number of delay symbols

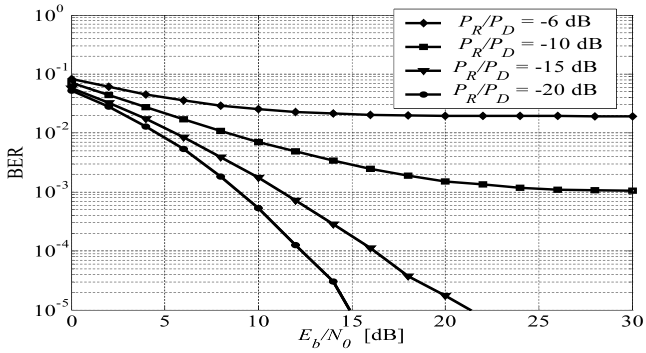

(a) 3-path

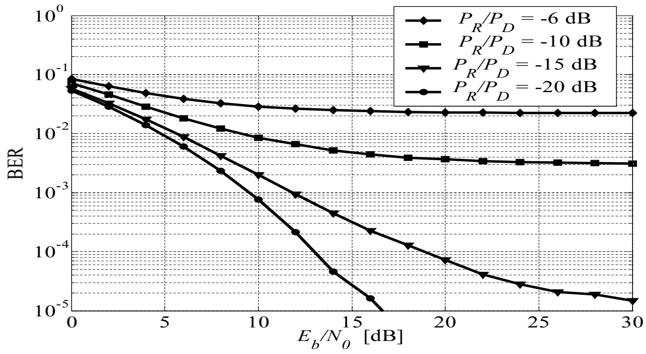

(b) 4-path

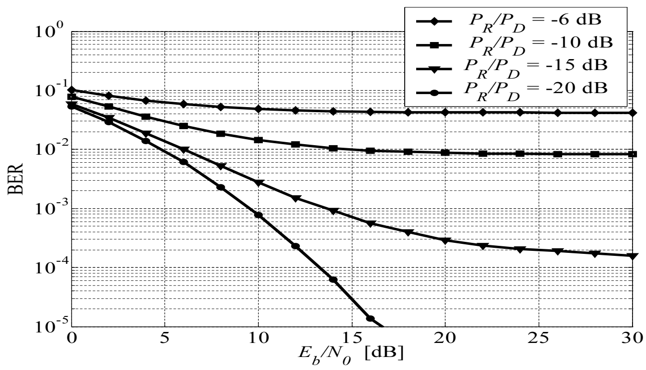

(c) 5-path

Fig. 5.9 BER characteristics for 3, 4, and 5-path

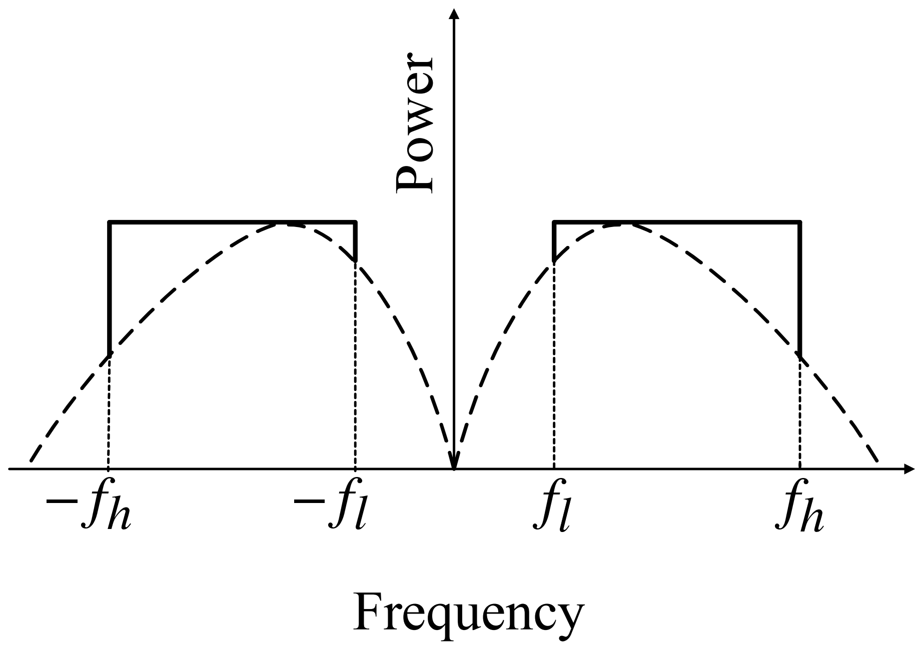

(a) Channel equalisation

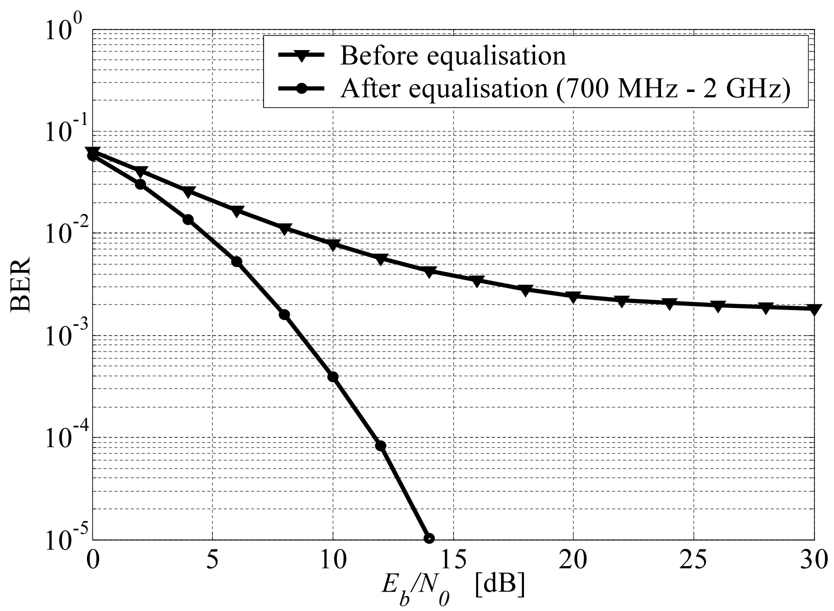

(b) BER characteristics

Fig. 5.10 Channel equalisation and the BER characteristics

Chapter 6

WBT Transmission Model and DC-balanced Codes

We discuss some aspects of the transmission model for WBT. In particular, the relationship between pulse widths and antenna bandwidths are considered in terms of the BER using computer simulations. The comparison of DC-balanced codes (such as CMI, DMI, Manchester, Miller, and NRZ-AMI) is also described.

6.1 Transmission Model based on Friis' Transmission Formula

A certain transmission model is required to evaluate the relationship between pulse widths and antenna bandwidths in terms of the BER using computer simulations. An extremely wide bandwidth is needed in the wireless baseband transmission because baseband pulses are radiated directly. Thus, in a practical wireless baseband transmission, an antenna could be treated as a band-pass-filter (BPF). To estimate the necessary bandwidth, a -6 dB/octave model, shown in Fig. 6.1, is assumed as the transmission model, including transmitting and receiving antennas, where f_l is the lower limit of the pass band and f_h is the upper limit of the pass band. The reason for selecting -6 dB/octave is the relationship with Friis' transmission formula [33, 34], assuming that the gain of the transmitting antenna and that of the receiving antenna are kept constant in the operational frequency range. This was approximately supported by our measurement, as shown in Fig. 4.5(a). The formula is given as

$$P_r = \frac{\lambda^2 P_t G_t G_r}{(4\pi d)^2} \propto \frac{1}{f^2}, \tag{6.1}$$

where P_r is the received power, P_t is the transmitted power, G_t is the transmitting antenna gain, G_r is the receiving antenna gain, λ is the wavelength, and d is the distance between the transmitting and receiving antennas. When assuming G_t, G_r are constant with respect to frequency, a frequency of twice the magnitude reduces the received power to one-quarter of the original value, as indicated by Eq. (6.1). This is a physical limitation of wide-band omni-directional antennas in which the relationship between antenna gains for transmission and reception are kept constant in the operational frequency range [32, 35]. The phase characteristic for the -6 dB/octave model is assumed to a linear phase characteristic. In particular, we set 0 phase in computer simulations. Although we omit the distance component d in Eq. (6.1) under this discussion, the radiated electromagnetic field strength is decreased at the rate of $1/d$, or the received power is decreased at the rate of $1/d^2$ in actual communications at far electromagnetic-fields indicated in the right side of Eq. (6.1). Figure 6.2 indicates an output waveform of Manchester encoding using the -6 dB/octave model at $f_l = 50$ MHz, and $f_h = 1,000$ MHz. Comparing Fig.

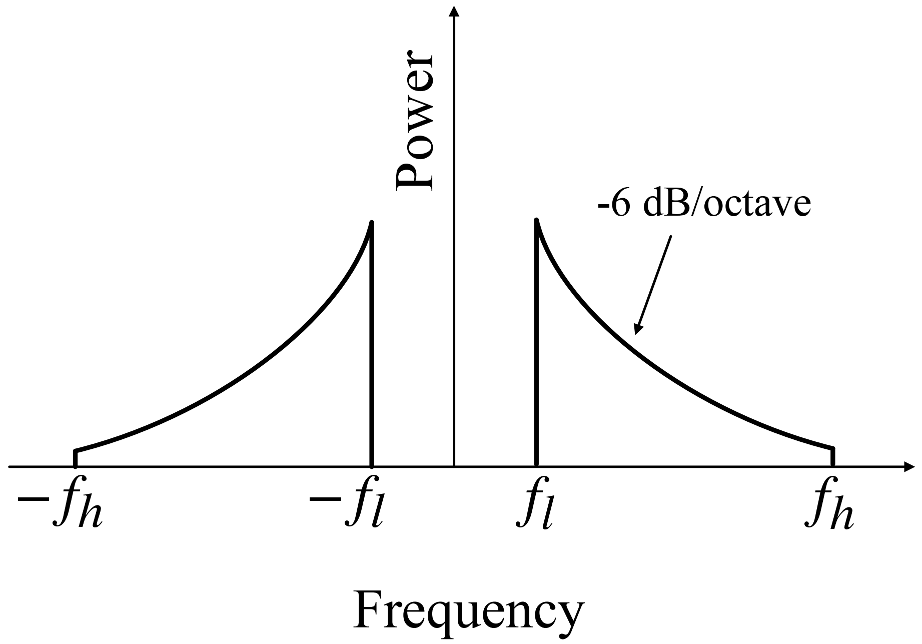

Fig. 6.1 Wireless baseband transmission model based on Friis' transmission formula

4.6(b) and Fig. 4.9(a) with Fig. 6.2, we find that a similar waveform is obtained using the −6 dB/octave model. The above results indicate the appropriateness of the −6 dB/octave model.

6.1.1 Parameters f_l and f_h in Computer Simulations

For the calculations, we set f_l and f_h as follows. The power spectrum of a Manchester encoded signal is shown in Fig. 6.3. Here, we normalise the frequency f with the pulse width T_0 shown in Fig. 6.3 as fT_0, which is used hereinafter. Since the effect of transmission quality in $f_hT_0 > 1$ must be negligible, as shown in Fig. 6.3, we fixed the upper frequency f_hT_0 to 1. Although a lower frequency f_lT_0 near the DC (direct current) is desirable, we set $f_lT_0 = 0.1$ as the initial value taking

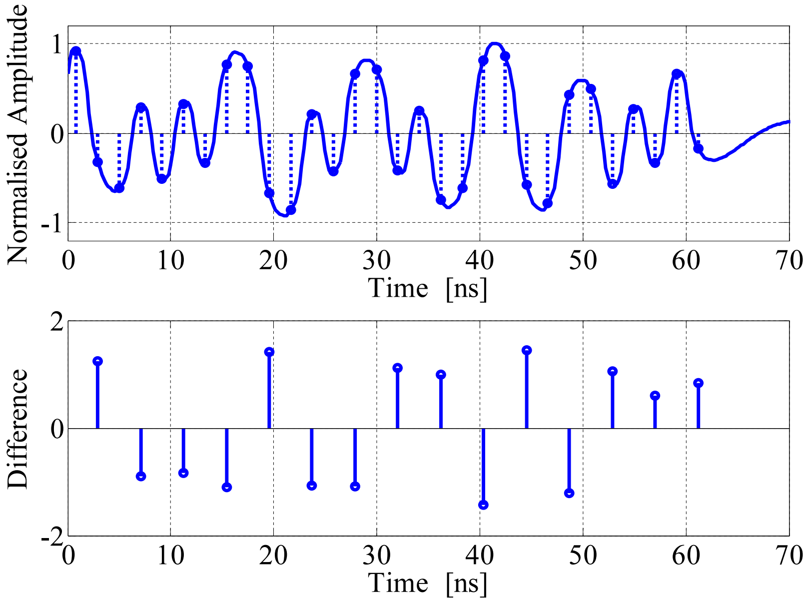

Fig. 6.2 Output waveform of Manchester encoding using the -6dB/octave model

the actual antennas into account.

6.1.2 Required Antenna Bandwidth

We estimate the required antenna bandwidth for the wireless baseband transmission using Manchester encoding. First, we varied $f_l T_0$ from 0.1 to 0.4 while fixing $f_h T_0$ to 1. The result is shown in Fig. 6.4. We also plotted $f_l T_0 = 0.07$ in Fig. 6.4 as the reference, which is the best performance limit because there is no difference between $f_l T_0 = 0.07$ and $f_l T_0 = 0.1$. Although the BER is less than 10^{-4} at a S/N of over 12dB in $f_l T_0 = 0.1$ and 0.2, error-floors appear in $f_l T_0 = 0.3$ and 0.4. We can therefore state that the required $f_l T_0$ is smaller than 0.2 for wireless baseband transmission using Manchester encoding. Next, we varied $f_h T_0$ from 0.7 to 0.4, while fixing $f_l T_0$ to 0.1. The result is shown in Fig. 6.5. We also plotted

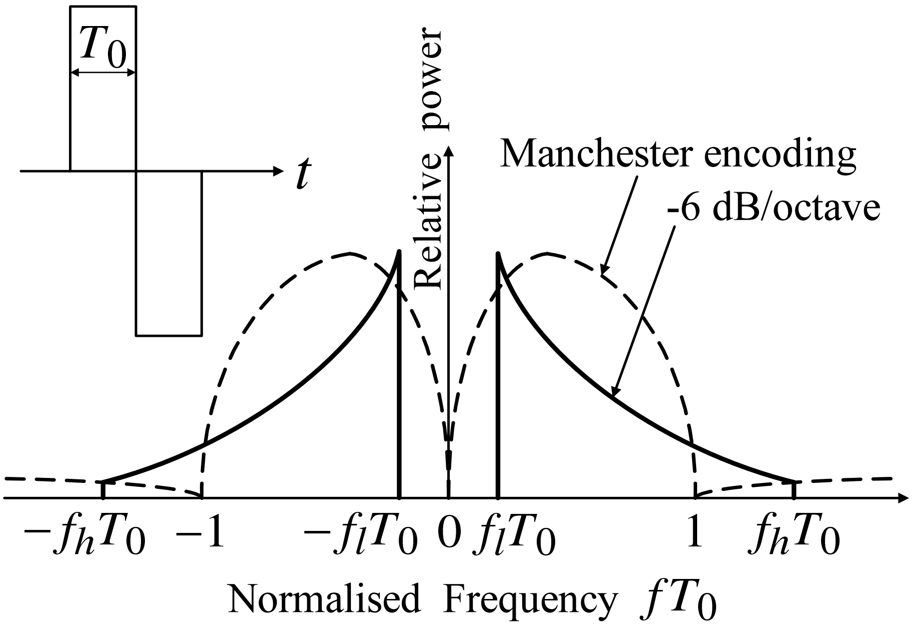

Fig. 6.3 Power spectrum of a Manchester encoded signal

$f_hT_0 = 1$ as the reference. From Fig. 6.5, we can state that the required f_hT_0 is over 0.6. That is, from the above results, we determined that the required f_lT_0 to be under 0.2 and f_hT_0 to be over 0.6. Finally, we examined the influence on fractional bandwidth B_f with fixed centre frequency f_c and T_0. Here, B_f is defined as follows:

$$B_f = \frac{f_h - f_l}{f_c} = \frac{2(f_h - f_l)}{f_h + f_l}. \tag{6.2}$$

We fixed f_c to 0.4, taking into account the previous result in which f_l is less than 0.2 and f_h is greater than 0.6, and fixed T_0 to 1. Pairs of f_l and f_h were varied as 0.3–0.5 ($B_f = 0.5$), 0.2–0.6 ($B_f = 1$), and 0.1–0.7 ($B_f = 1.5$), respectively. Figure 6.6 shows the results. Figure 6.6 indicates that wireless baseband transmission is realisable using Manchester encoding with approximately $B_f \geq 1$ antennas,

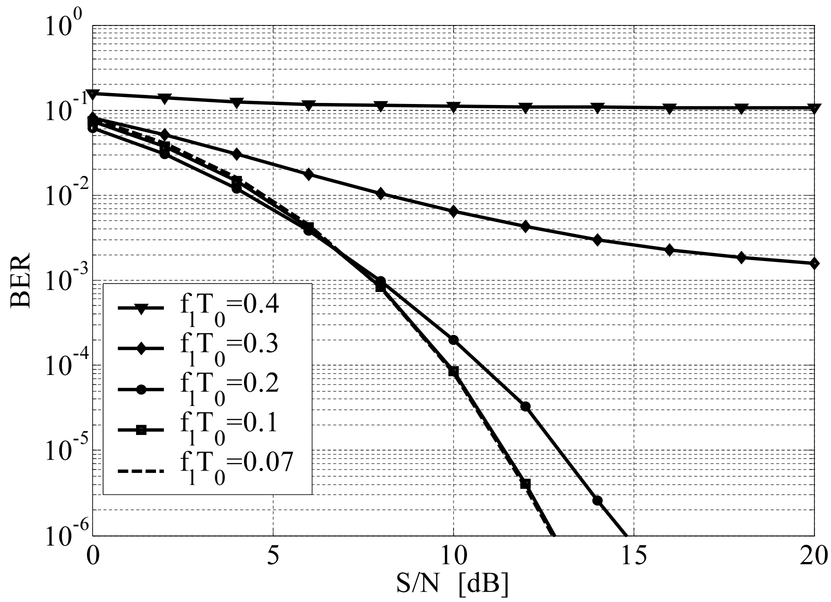

Fig. 6.4 BER for varying $f_l T_0$ in computer simulations ($f_h T_0 = 1$)

because the error-floor does not appear and a BER of 10^{-4} is achieved in $B_f = 1$ and $B_f = 1.5$. Considering our discone antenna, the requirement ($B_f \geq 1$) is satisfied because B_f is 1.4 (as mentioned in 4.3).

The following is a summary of our above discussions.

- Assuming that there is an antenna with centre frequency f_c and fractional bandwidth $B_f \geq 1$, wireless baseband transmission is possible with $T_0 \approx 1/2 f_c$ using the Manchester encoding scheme.

- The transmission rate is approximately f_c bps, because Manchester encoding makes $2T_0$ a 1-bit transmission.

- The characteristic of our handmade discone antennas is equivalent to $2 f_c \simeq$ 500 MHz (as shown in Fig. 4.4 and Fig. 4.5), which indicates a 250 Mbps

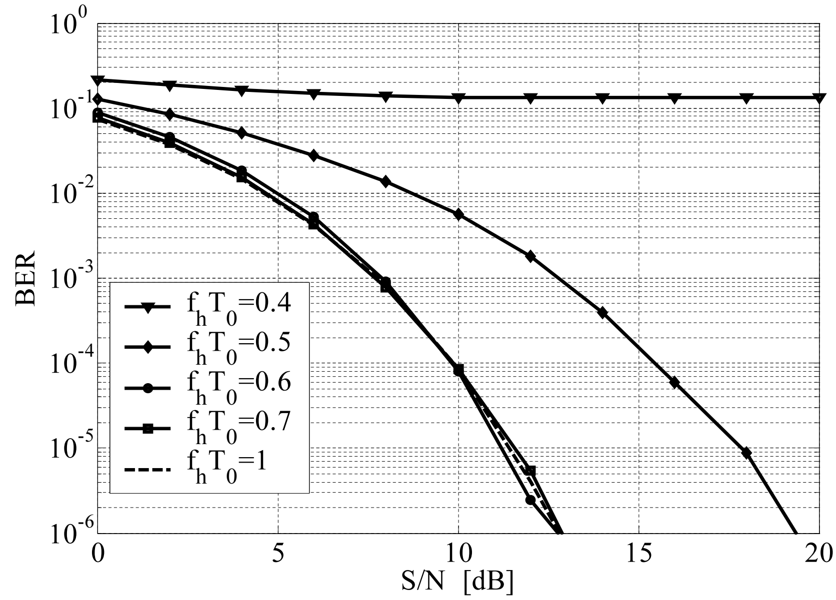

Fig. 6.5 BER for varying $f_h T_0$ in computer simulations ($f_l T_0 = 0.1$)

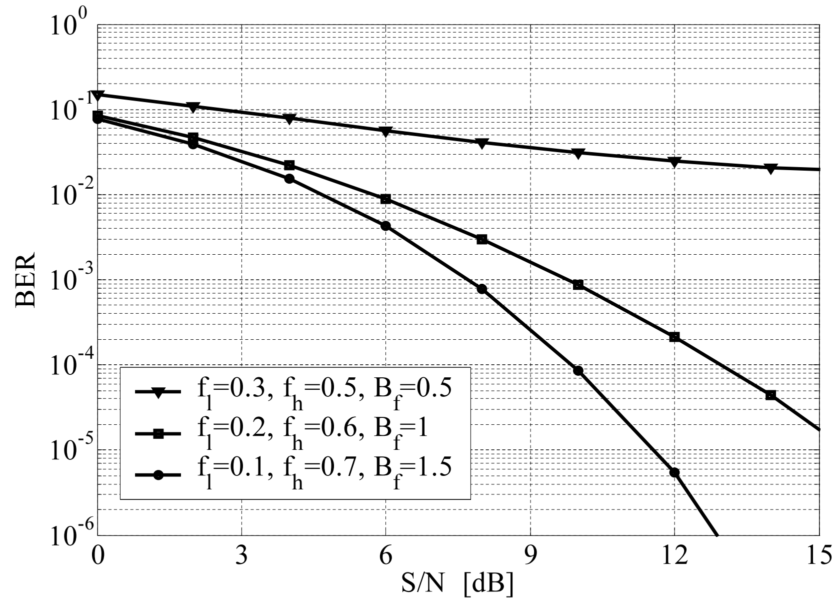

Fig. 6.6 BER for varying B_f in computer simulations ($f_c = 0.4$)

WBT as shown in Fig. 4.6.

- When we consider a scale model, WBT with some volume antennas
  - $(1\ \mathrm{m})^3 \rightarrow 250$ Mbps (our discone antenna)
  - $(10\ \mathrm{cm})^3 \rightarrow 2.5$ Gbps
  - $(1\ \mathrm{cm})^3 \rightarrow 25$ Gbps

  are expected using Manchester encoding.

6.2 Comparison of DC-balanced Codes

6.2.1 CMI, DMI, Manchester, Miller, and NRZ-AMI Codes

We compare some DC-balanced codes in WBT. The DC-balanced line codes are CMI (coded mark inversion), DMI (differential mode inversion), Manchester, Miller, and NRZ-AMI (non return to zero-alternate mark inversion). Fig. 6.7 shows the codes. The spectrum for these codes are shown in Fig. 6.8. We also show the relationship between S_{21} and Manchester spectrum in Fig. 6.9. DMI and NRZ-AMI show the same characteristic in Fig. 6.8. Although Miller code has a few DC-component, the quantity must be negligible. Therefore, we compare five DC-balanced codes including Miller code. Further description on line codes are given in the reference [36].

The evaluation method is the same as mentioned in 4.5.1 (VNA-PC method). We choose the minimum pulse width (not T_s) as 0.2 ns. Therefore, the transmission rate is 5 Gbps ($Ts = 0.2$ ns) for NRZ-AMI, and 2.5 Gbps ($Ts = 0.4$ ns) for

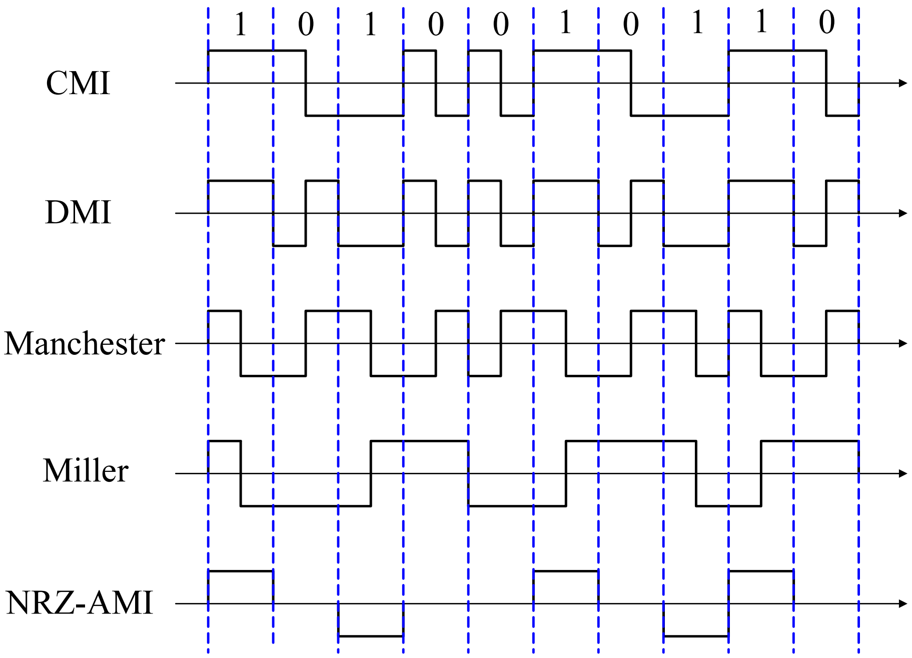

Fig. 6.7 DC-balanced codes

other codes. The experimental environment is the same as Fig. 5.3.

6.2.2 Result

Fig. 6.10 indicate the result for comparing DC-balanced codes. We also plotted the BPSK theoretical curve in Fig. 6.10(a) and Fig. 6.10(b) In Fig. 6.10(a), an almost same characteristic is obtained excluding NRZ-AMI. In Fig. 6.10(b) and Fig. 6.10(c), Manchester superior to other codes. We consider that the dominant factor on the BER performance is the detection method. Manchester can be detected the difference of two sampling point and the amplitude value on sampling point itself is not related with detection result (0 or 1). On the other hand, other codes shown in Fig. 6.7 need to read the amplitude itself exactly for a threshold value.

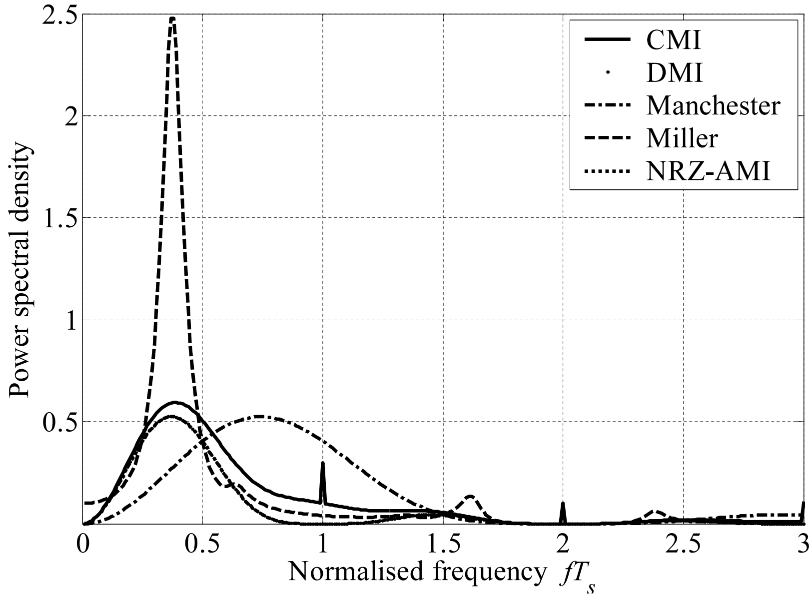

Fig. 6.8 Spectrum for DC-balanced codes (T_s is symbol period)

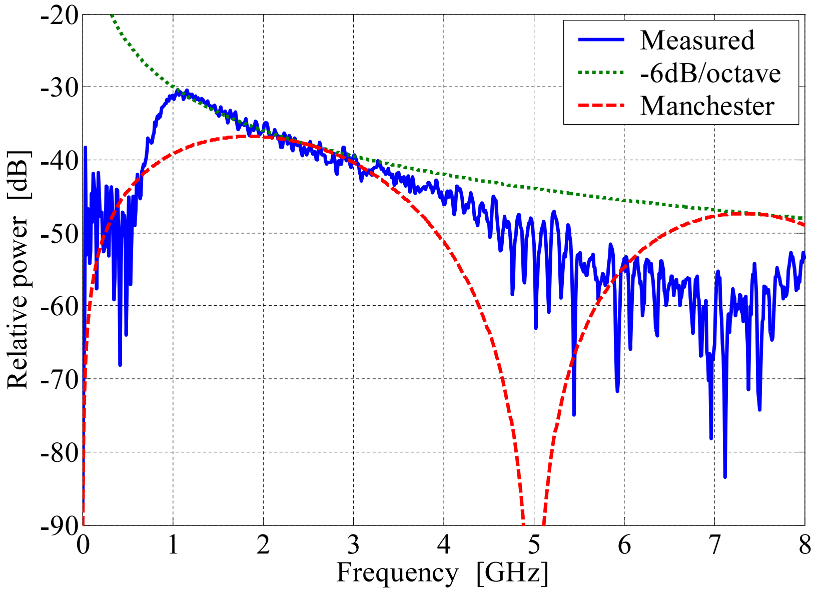

Fig. 6.9 S_{21} and Manchester spectrum (2.5 Gbps)

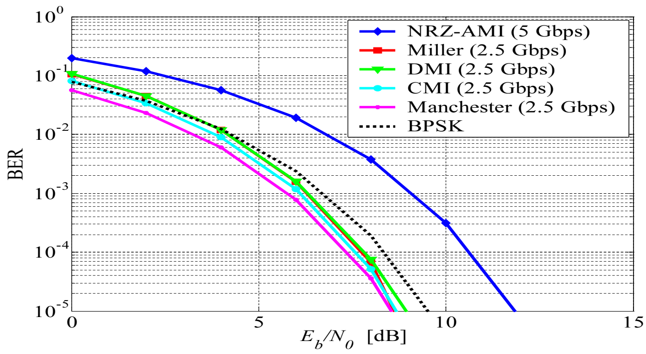

(a) Ideal

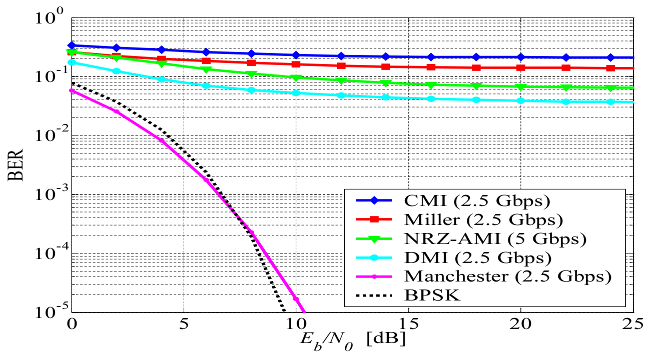

(b) Free space (effected by antenna characteristic)

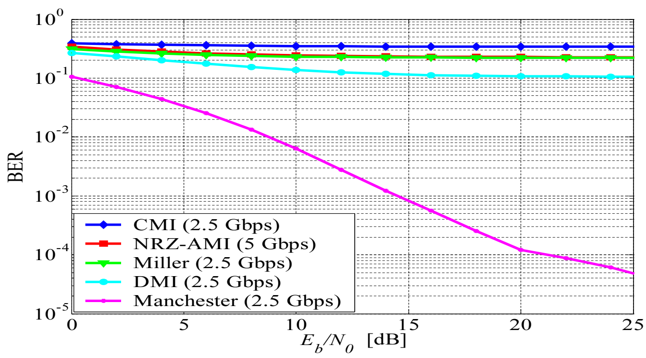

(c) Multipath

Fig. 6.10 BER characteristics for CMI, DMI, Manchester, Miller, and NRZ-AMI codes

Manchester encoding is one of the suitable encoding schemes for WBT as shown in Fig. 6.10. Assuming that we can decrease transmission rate less than 1/2 (Manchester halves the data tate), there might be still better encoding schemes. However, we would not like to decrease data transmission rate and would like to use a simple encoding scheme. Manchester encoding will be the best candidate for that requirements.

Chapter 7

Topics in WBT

We have carried out WBT experiments because we would like to investigate the fundamental capabilities and characteristics. Although we do not suppose specific applications of this wireless baseband transmission for the reason, still considering practical application systems, this system might be a candidate for effective use of millimetre or sub-millimetre wave regions, which have extremely wide bandwidths for high-speed (such as 100 Gbps) wireless transmissions. Furthermore, interference problems are mitigated in that regions because millimetre electromagnetic waves are attenuated rapidly in the atmosphere by water vapour and oxygen. Such a communication using near electromagnetic-fields might also be suitable as application systems of this system.

7.1 Channel Capacity

We calculate channel capacity to seek applications for WBT. We use the value UWB Japan standard[1] as one example. Fig. 7.1 indicates channel capacity for

[1]Tx power is -41.3 dBm/MHz and the frequency ranges are 3.4 – 4.8 GHz and 7.25 – 10.25 GHz. We use 3 GHz as the bandwidth considering the latter case.

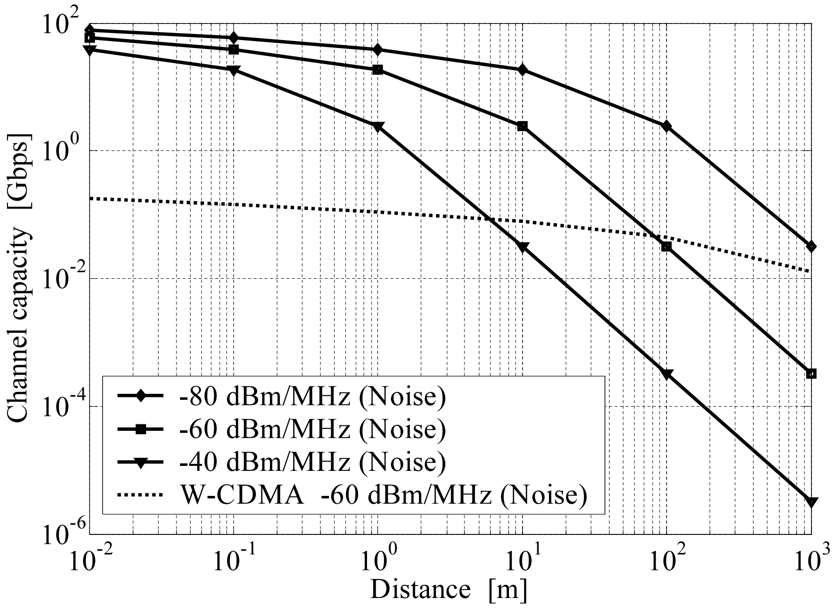

Fig. 7.1 Channel capacity

various conditions. These curves can be calculated from Shannon's channel capacity theorem;

$$C = W \log_2 \left(1 + \frac{S}{N}\right), \tag{7.1}$$

where W is a bandwidth. We also plotted W-CDMA (wideband code division multiple access)[2] as an example of typical wireless systems. There is clear evidence that a wideband system including WBT has an advantage over short-distance (up to 10 m) communications. Fig. 7.2 shows an application of WBT.

[2]Tx power is 24 dBm and W is 5 MHz.

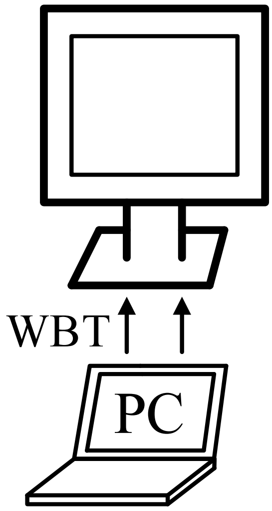

Fig. 7.2 Laptop PC and display

7.2 System

7.2.1 Transceiver architecture

WBT architecture is shown in Fig. 7.3. The construction becomes simpler than conventional wireless systems because it is possible to omit oscillation circuits and mixers which are used for frequency conversions shown in Fig. 7.3. Furthermore, this reduction makes low-power operation possible.

7.2.2 PAPR (peak-to-average power ratio)

The PAPR (peak-to-average power ratio) of WBT is almost 1. This is advantage comparing IR (impulse radio). IR has a high PAPR and this means that a excessive PA (power amplifier) comparing its effective output power. However, such a PA is not needed in WBT.

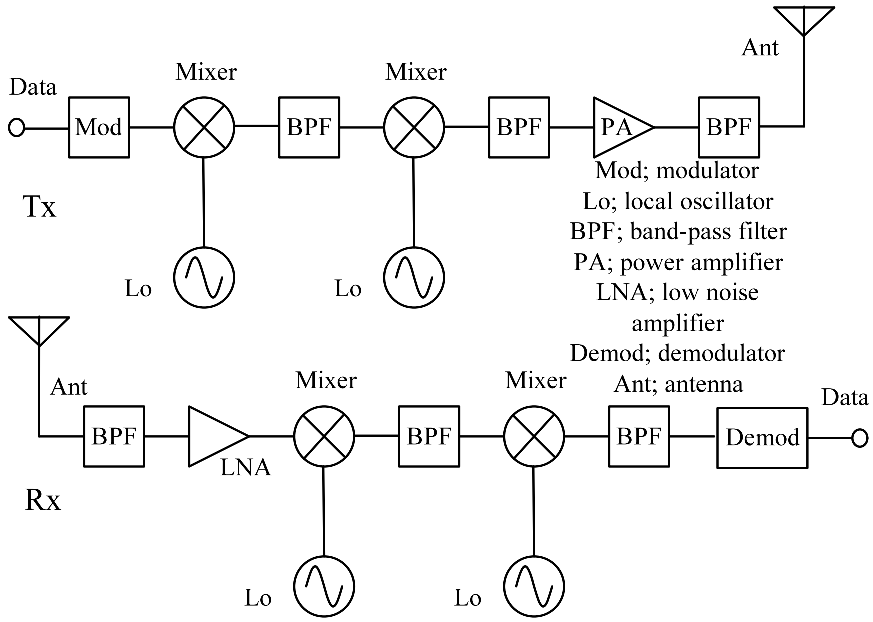

(a) Conventional wireless system

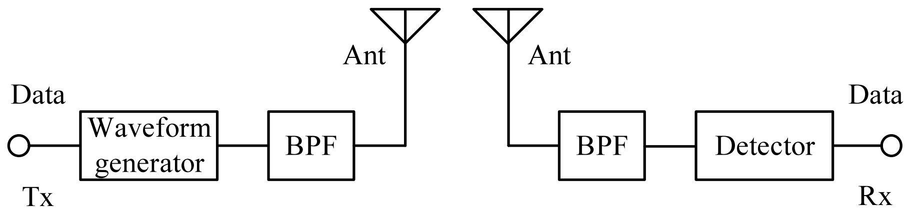

(b) Wireless baseband transmission system

Fig. 7.3 Transceiver architecture

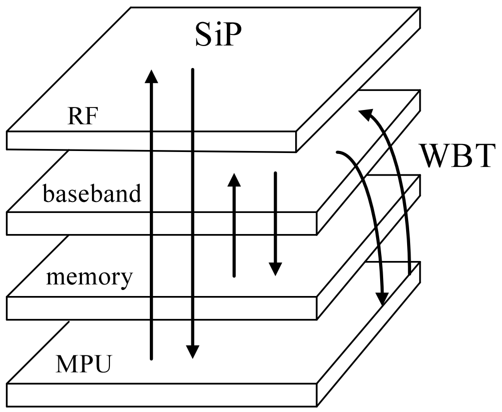

Fig. 7.4 Inter-chip communications

7.3 Near Electromagnetic-fields Communications

Although we have treated far electromagnetic-fields in this paper, applications of the near electromagnetic-fields would be performed using WBT technologies. In particular, a wireless communication at the order of μm, such as micro-machine-to-micro-machine and the instead of wiring in semiconductors, must seek a new wireless transmission techniques. Fig. 7.4 shows such an example.

7.4 Effective Use of Array – MIMO (multiple input multiple output)

Considering that more high-speed transmissions of WBT, the effective use of space is a candidate. To be able to use space is a merit of wireless transmissions and WBT is also not exceptional. Figure 7.5 indicates 2x2 (the number of Tx antenna is 2 and the number of Rx one is also 2) MIMO system. We measured channel matrix eigenvalues on a WBT-MIMO system. One channel matrix eigenvalue corresponds to the one equivalent transmission path. Experimental

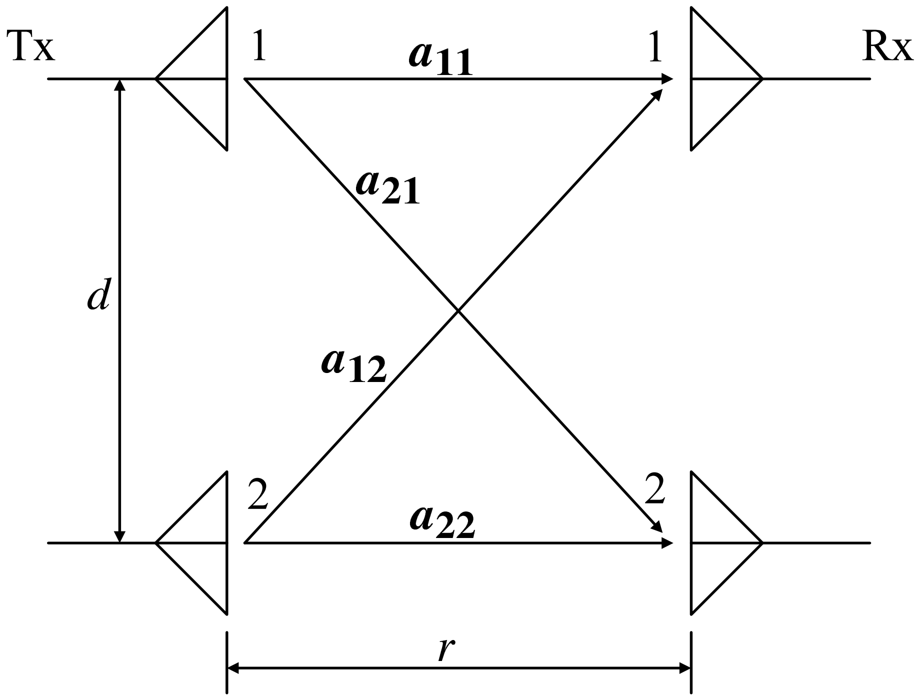

Fig. 7.5 2x2 MIMO

condition is the same as Chapter 5. In Fig. 7.5, we kept r as 1 m and changed d as 0.25 and 1 m. Figure 7.6 shows the channel matrix eigenvalues λ_1 and λ_2 for 2x2 WBT-MIMO in free space. A 2x2 MIMO system has generally two practical eigenvalues in multipath environment although only one practical eigenvalue is appeared in free space. This difference depends on the relationship between d and r which are shown in Fig. 7.6.

7.5 SDR (software defined radio)

The architecture of WBT transceivers consists of almost all digital circuits as shown in Fig. 7.3. This means that WBT gets along with software defined radio (SDR). Because analogue circuits such as oscillators and mixers do not need

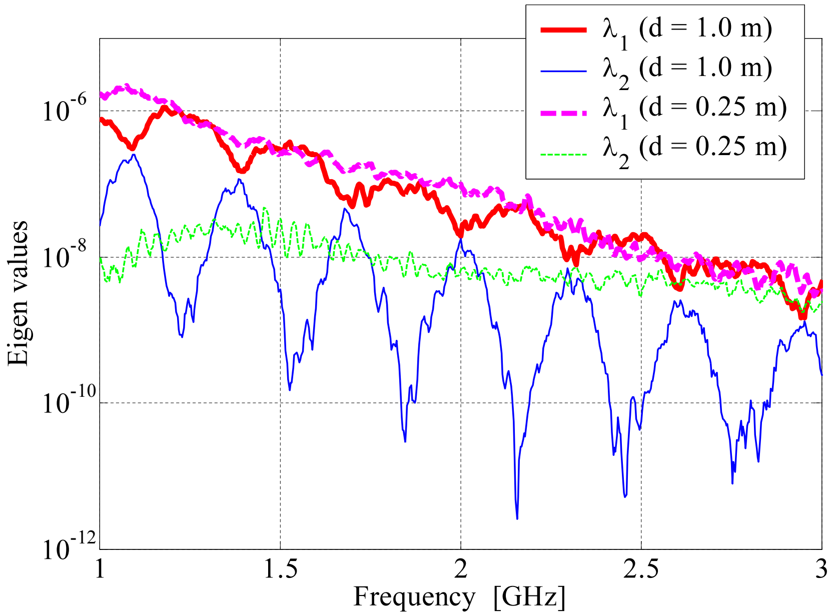

Fig. 7.6 Eigenvalue characteristics for WBT-MIMO in free space

to make a WBT transceiver and the high-speed processors, A/D (analogue-to-digital converter), and D/A (digital-to-analogue converter) are required. A WBT transceiver will be made in the near future using SDR technology.

Chapter 8

Conclusion

A baseband transmission scheme for wireless communications has been proposed and examined experimentally with respect to feasibility. We found that when using an antenna with a flat amplitude spectrum and a linear phase characteristic over a given band (such as discone antenna) and an appropriate encoding scheme (such as Manchester encoding), WBT is realisable. We have confirmed 250 Mbps and 2.5 Gbps WBT transmissions using measured frequency-domain channel characteristics.

An analysis method of real signals has been described to evaluate transmission characteristics; i.e., BER. Signal analysis in conventional wireless systems is usually performed on the equivalent low-pass system and the signal has complex-valued. However, the WBT signal can not be analysed in the equivalent low-pass system because of having no sinusoidal carrier-waves. Therefore, it is required for WBT to make an analysis method which is based on real signal analysis. We made, therefore, a real signal analysis method to obtain BER. One can use this method not only WBT but also other systems. An transmission model;

-6 dB/octave model has been made to calculate the relationship between an antenna bandwidth and an pulse width. As the result, the required fractional bandwidth (max value is 2) for an antenna is 1 and the data rate equals to the centre frequency of the antenna.

Transmission characteristics in multipath environments are evaluated using the real signal analysis method with measured channel characteristics. BER characteristics are calculated on computers with varying reflection coefficients of reflected waves, the number of delayed symbols, the power ratio between a direct wave and reflected waves, and the number of reflected waves. The result makes it clear that the dominant factor for BER is the power ratio between a direct wave (P_D) and reflected waves (P_R). A practical WBT communication can perform even in multipath environments when P_R/P_D is smaller than -15 dB without equalisation and error correcting techniques.

Although we do not suppose specific applications for this WBT, considering practical application systems, short-distance (e.g., up to 10 m) communications match WBT. The reason is self-evident considering Shannon's channel capacity theorem. WBT might also be applicable to communication systems using near electromagnetic-fields such as inter-chip communications, although we treat only far one in this paper.

We believe that WBT is to be another wireless transmission scheme.

References

[1] B. Komiyama, “Introduction to the contents of research at ATR Adaptive Communications Research Laboratories,” ATR Journal, vol.23, pp.7–10, June 1996.

[2] G. R. Aiello and G. D. Rogerson, “Ultra-wideband wireless systems,” IEEE Microw. Magazine, vol.4, no.2, pp.36–47, June 2003.

[3] D. Porcino and W. Hirt, “Ultra-wideband radio technology: Potential and challenges ahead,” IEEE Commun. Mag., vol.41, no.7, pp.66–74, July 2003.

[4] K. Araki, “RF and high-speed circuits for ultra-wideband technology,” Microwave Workshops and Exhibition, TL05-01, Yokohama, Japan, Nov. 2003.

[5] T. Kobayashi and S. Kouya, “Overview of research and development in ultra wideband wireless systems,” IEICE Trans. Fundamentals (Japanese Edition), vol.J86-A, no.12, pp.1264–1273, Dec. 2003.

[6] R. Kohno, “Collaboration among industry, academia and government for R & D of ultra wideband wireless technologies and contribution in standard-

ization in wireless PAN," IEICE Trans. Fundamentals (Japanese Edition), vol.J86-A, no.12, pp.1274–1283, Dec. 2003.

[7] S. Roy, J.R. Foerster, V.S. Somayazulu, and D.G. Leeper, "Ultrawideband radio design: The promise of high-speed, short-range wireless connectivity," Proc. IEEE, vol.92, no.2, pp.295–311, Feb. 2004.

[8] R. J. Fontana, "Recent system applications of short-pulse ultra-wideband (UWB) technology," IEEE Trans. Microw. Theory Tech., vol.52, no.9, pp.2087–2104, Sept. 2004.

[9] T. K. Sarkar, R. J. Mailloux, A. A. Oliner, M. Salazar-Palma, and D. L. Sengupta, History of Wireless, Wiley-Interscience, NJ, 2006.

[10] M. Z. Win and R. A. Scholtz, "Impulse radio: How it works," IEEE Commun. Lett., vol.2, no.2, pp.36–38, Feb. 1998.

[11] M. Z. Win and R. A. Scholtz, "Ultra-wide bandwidth time-hopping spread-spectrum impulse radio for wireless multiple-access communications," IEEE Trans. Commun., vol.48, no.4, pp.679–691, April 2000.

[12] R. Forster, "Manchester encoding: Opposing definitions resolved," IEE Engineering Science and Education Journal, vol.9, no.6, pp.278–280, Dec. 2000.

[13] C. L. Bennett and G. F. Ross, "Time-domain electromagnetics and its applications," Proc. IEEE, vol.66, no.3, pp.299–318, March 1978.

[14] G. F. Ross, “The transient analysis of certain TEM mode four-port networks,” IEEE Trans. Microw. Theory Tech., vol.14, no.11, pp.528–542, Nov. 1966.

[15] G. F. Ross, “A time domain criterion for the design of wideband radiating elements,” IEEE Trans. Antennas Propag., vol.16, no.3, pp.355–356, May 1968.

[16] G. F. Ross, “Transmission and reception system for generating and receiving base-band duration pulse signals without distortion for short base-band pulse communication system,” U.S. Patent 3,728,632, April 17, 1973.

[17] H. F. Harmuth, “Transmission of information by orthogonal time functions,” Trans. of the AIEE Pt.I Commun. and Electronics, vol.79, pp.248–255, July 1960.

[18] H. F. Harmuth, Transmission of Information by Orthogonal Functions, Springer-Verlag, New York, 1969.

[19] H. F. Harmuth, Transmission of Information by Orthogonal Functions, Second ed., Springer-Verlag, New York, 1972.

[20] H. F. Harmuth, Sequency Theory — Foundations and Applications, Academic Press, New York, 1977.

[21] H. F. Harmuth, Nonsinusoidal Waves for Radar and Radio Communication, Academic Press, New York, 1981.

[22] H. F. Harmuth, Antennas and Waveguides for Nonsinusoidal Waves, Academic Press, New York, 1984.

[23] H. F. Harmuth, Propagation of Nonsinusoidal Electromagnetic Waves, Academic Press, New York, 1986.

[24] H. F. Harmuth, Radiation of Nonsinusoidal Electromagnetic Waves, Academic Press, New York, 1990.

[25] H. F. Harmuth, "A generalized concept of frequency and some applications," IEEE Trans. Inform. Theory, vol.14, no.3, pp.375–381, May 1968.

[26] H. F. Harmuth, "Selective reception of periodic electromagnetic waves with general time variation," IEEE Trans. Electromagn. Compat., vol.19, no.3, pp.137–144, Aug. 1977.

[27] H. F. Harmuth, "Frequency-sharing and spread-spectrum transmission with large relative bandwidth," IEEE Trans. Electromagn. Compat., vol.20, no.1, pp.232–239, Feb. 1978.

[28] A. G. Kandoian, "Three new antenna types and their applications," Proc. IRE (Waves and Electrons), vol.34, no.2, pp.70W–75W, Feb. 1946.

[29] D. Lamensdorf and L. Susman, "Baseband-pulse-antenna techniques," IEEE Antennas Propag. Mag., vol.36, no.1, pp.20–30, Feb. 1994.

[30] C. C. Bantin, "Pulsed communications link between two dipoles," IEEE Antennas Propag. Mag., vol.44, no.5, pp.75–82, Oct. 2002.

[31] T. Maeda, “UWB antennas: Antenna and propagation technologies for ubiquitous ultra high speed wireless communications and perspectives,” IEICE Trans. Commun. (Japanese Edition), vol.J88-B, no.9, pp.1586–1600, Sept. 2005.

[32] H. Schantz, The Art and Science of Ultrawideband Antennas, Artech House, Norwood, MA, 2005.

[33] H. T. Friis, “A note on a simple transmission formula,” Proc. IRE, vol.34, no.5, pp.254–256, May 1946.

[34] J. Takada, S. Promwong, and W. Hachitani, “Extension of Friis’ transmission formula for ultra wideband systems,” IEICE Technical Report, WBS2003-8, MW2003-20, May 2003.

[35] L. J. Chu, “Physical limitations of omni-directional antennas,” J. Appl. Phys., vol.19, pp.1163–1175, Dec. 1948.

[36] F. Xiong, Digital Modulation Techniques, Second ed., Artech House, Norwood, MA, 2006.

[37] H. S. Black, Modulation Theory, Van Nostrand, New York, 1953.

Appendix A

Single Pulse Transmission Experiments

Transmission characteristics of a single pulse had been investigated at the beginning on this study. Because a baseband signal stream are composed of some single pulses, it is important for WBT to transmit the shape of a single pulse faithfully.

A.1 Setup

A schematic diagram of the experimental setup is shown in Fig. A.1. All experiments had been carried out in the radio anechoic chamber (the same as Chapter 4 and Chapter 5). We used the DG (DG2040) and the DSO (TDS714L) (do not used VNAs).

A.2 Antennas

A.2.1 Antennas

In wideband wireless transmissions such as WBT, an antenna is regarded as a filter. It is important for WBT to use what type of antennas. The three antennas

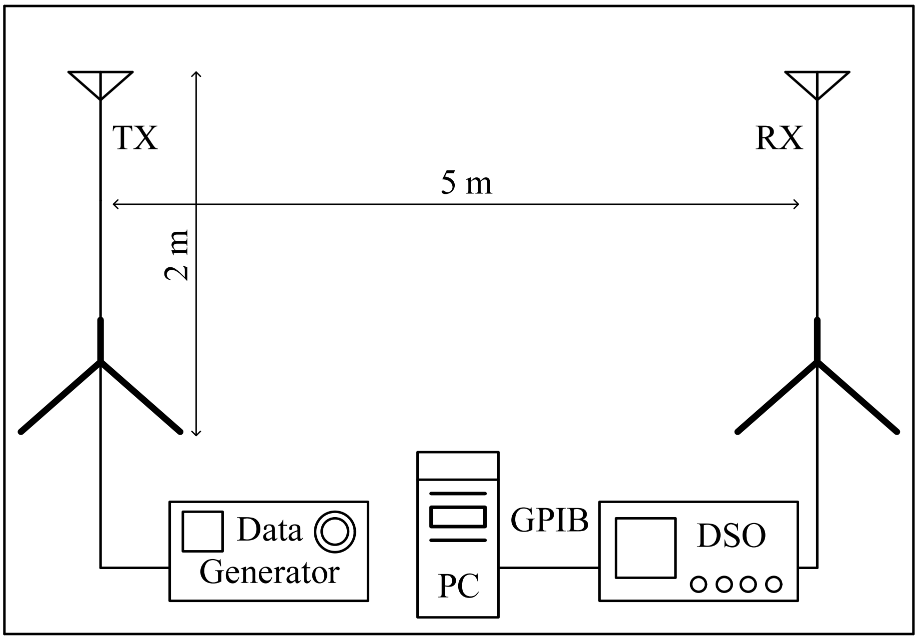

Fig. A.1 Experimental setup (in the radio anechoic chamber)

were used in the experiments.

- 1 m length dipole (handmade)
- Log periodic dipole array (LPDA) Creative Design CLP-5130-1
- 1 m length resistive-loaded dipole (handmade)

A dipole antenna is most fundamental in the antennas field. LPDA and resistive-loaded antennas are known as wideband antennas.

A.3 Method

A single pulse is generated at transmitter side by the DG and a received waveform is measured by the DSO. The pulse width of a single pulse is varied from 1 μs to 1 ns.

(a) Dipole

(b) LPDA

(c) Resistive loaded dipole

Fig. A.2 Antennas used in single pulse experiments

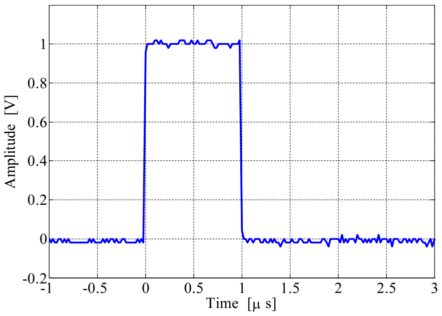

(a) 1 μs

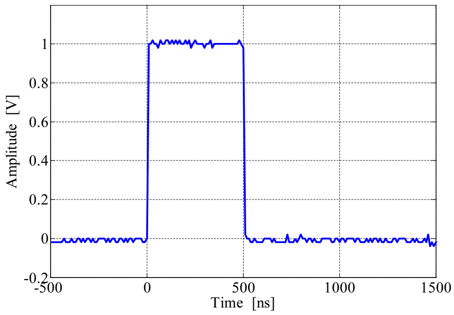

(b) 500 ns

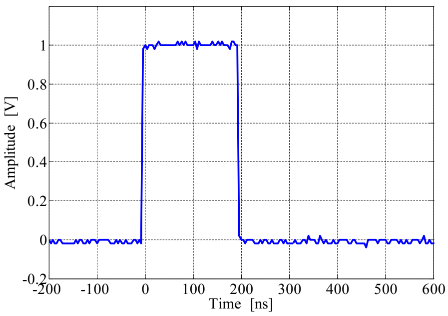

(c) 200 ns

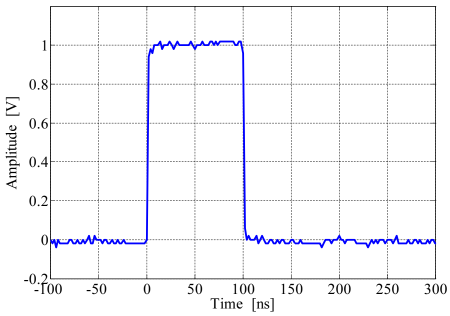

(d) 100 ns

Fig. A.3 Transmitting waveforms

A.4 Results

A.4.1 Unipolar Pulse

The transmitting unipolar pulses (output of the DG) are shown in Fig. A.3.

DSO Performance Limit

We can observe distorted waveforms below 20 ns in Fig. A.3. This effect is caused by the DSO performance limit. One main reason is the analogue bandwidth on the DSO. Note that the DG output has not distortions.

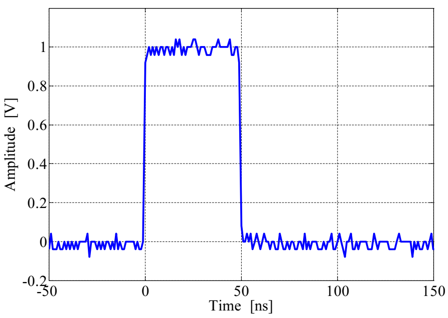

(e) 50 ns

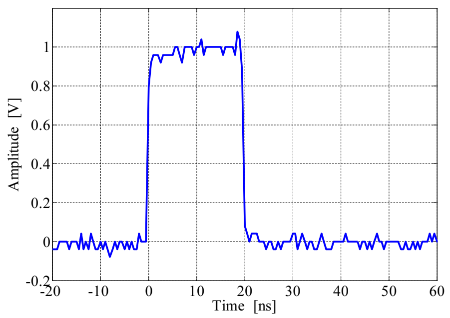

(f) 20 ns

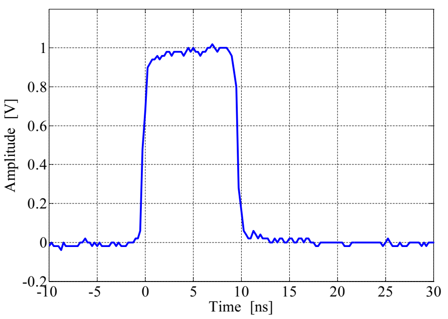

(g) 10 ns

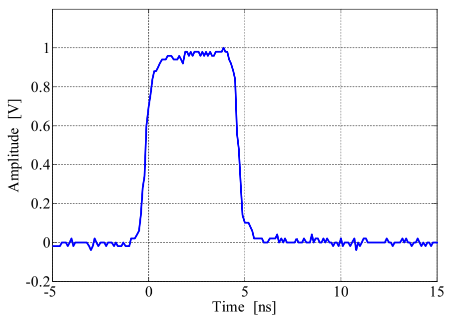

(h) 5 ns

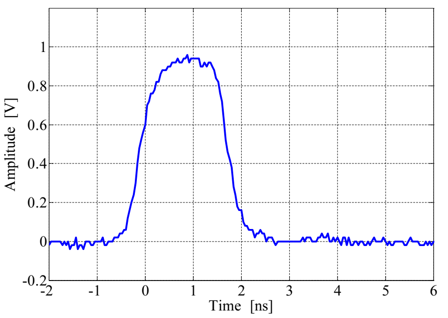

(i) 2 ns

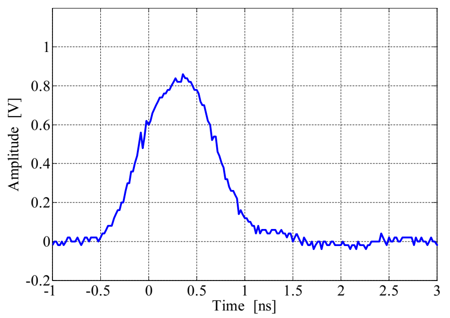

(j) 1 ns

Fig. A.3 Transmitting waveforms

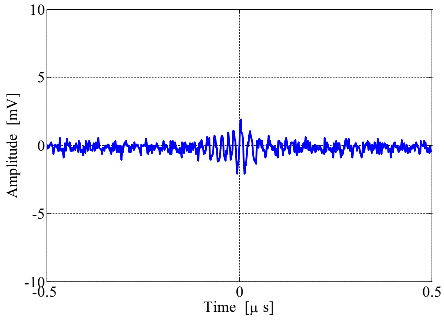

(a) 1 μs

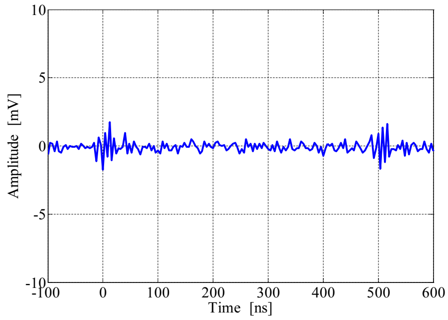

(b) 500 ns

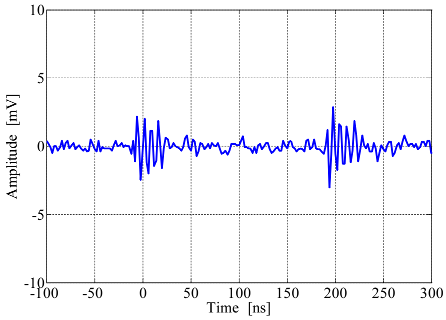

(c) 200 ns

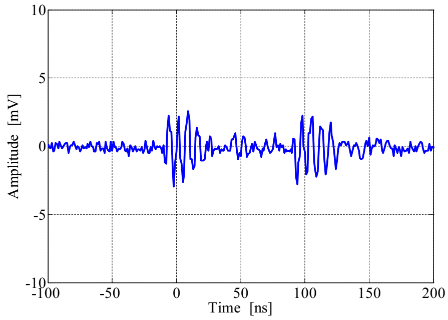

(d) 100 ns

Fig. A.4 Received waveforms for dipole antenna

Received Waveforms for Dipole Antenna

The received waveforms using the dipole antennas both the transmitter and receiver sides are shown in Fig. A.4. The ringing duration time is over ten times longer than the transmitting pulse width (e.g, Fig. A.3 (i) and Fig. A.4 (i)).

Received Waveforms for LPDA

The received waveforms using the LPDAs both the transmitter and receiver sides are shown in Fig. A.5. The ringing duration time is over twenty times longer than

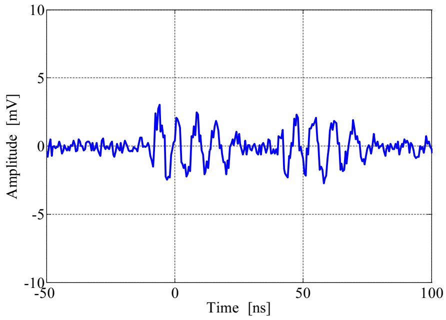

(e) 50 ns

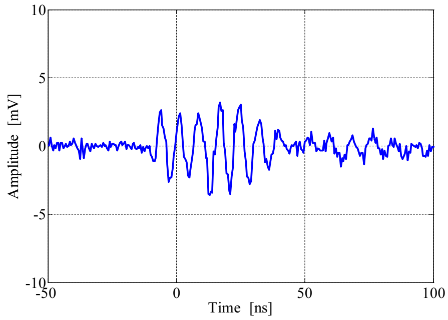

(f) 20 ns

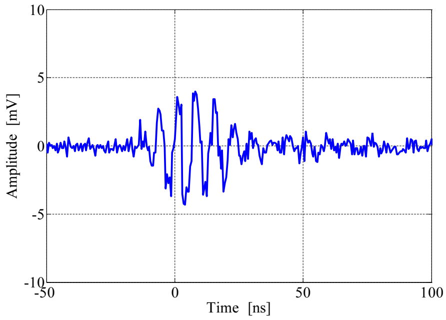

(g) 10 ns

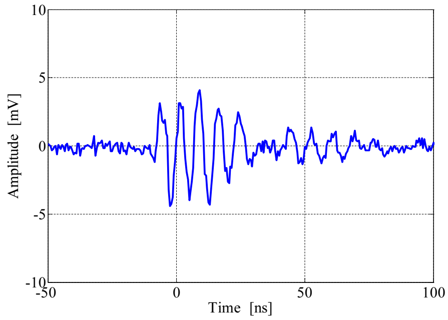

(h) 5 ns

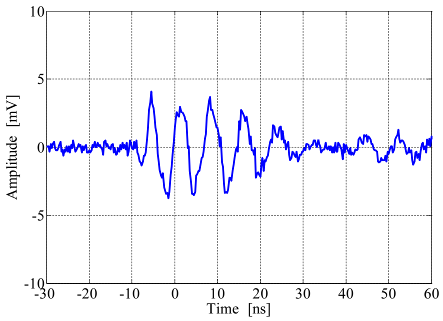

(i) 2 ns

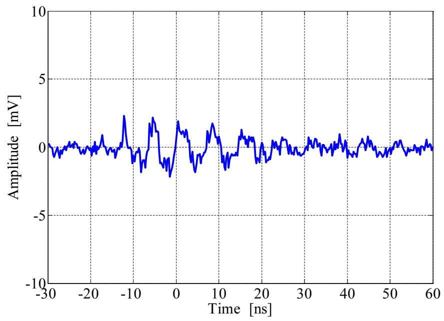

(j) 1 ns

Fig. A.4 Received waveforms for dipole antenna

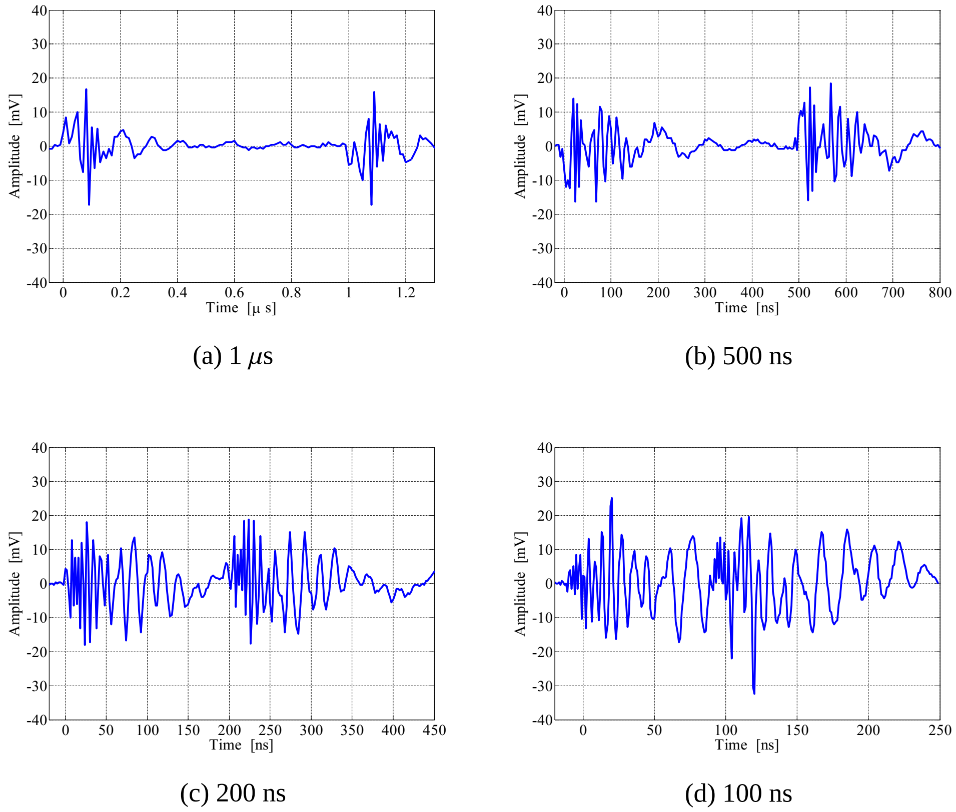

Fig. A.5 Received waveforms for LPDA

the transmitting pulse width (e.g, Fig. A.3 (i) and Fig. A.5 (i)).

Received Waveforms for Resistive-Loaded Dipole Antenna

The received waveforms using the resistive-loaded dipole antennas both the transmitter and receiver sides are shown in Fig. A.6. The received voltage could only measured at 2 ns; i.e., sufficient energy to observe by the DSO was not transmitted in other pulse widths. Comparing other antennas, although the ringing duration time is short, the resistive-loaded antenna can not transmit sufficient energy which

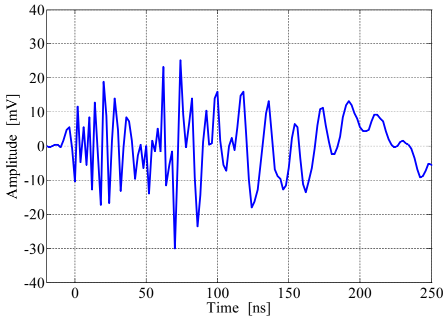

(e) 50 ns

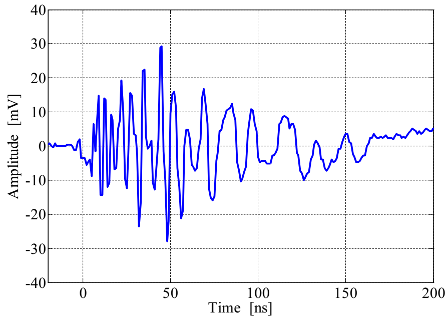

(f) 20 ns

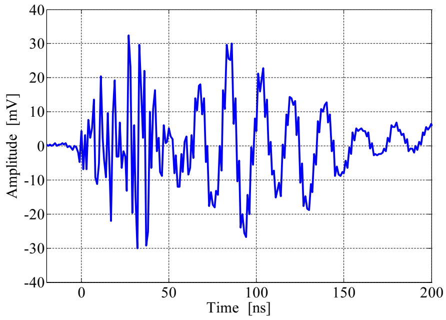

(g) 10 ns

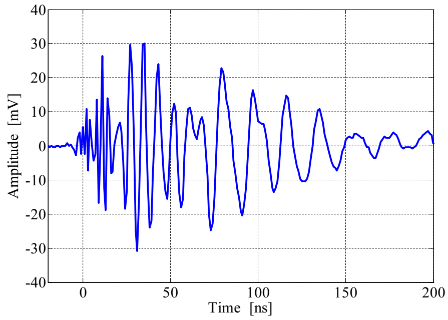

(h) 5 ns

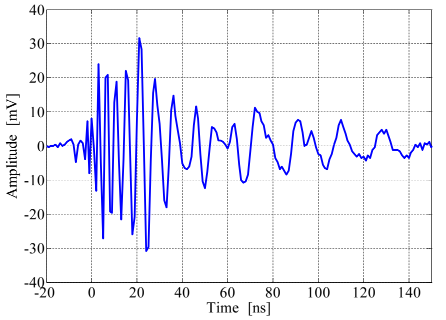

(i) 2 ns

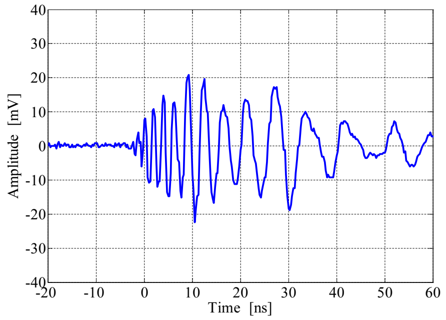

(j) 1 ns

Fig. A.5 Received waveforms for LPDA

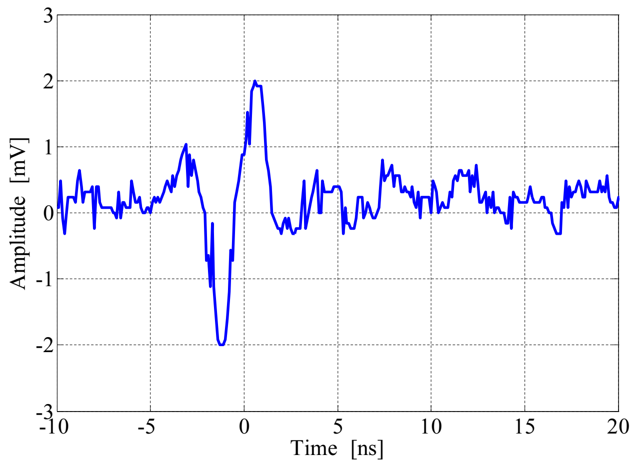

Fig. A.6 Received waveforms for a resistive-loaded dipole antenna (2 ns)

is needed in actual communications.

A.4.2 Polar Pulse

The transmitting polar pulses (output of the DG) are shown in Fig. A.7.

Received Waveforms for Dipole Antenna

The received waveforms using the dipole antennas both the transmitter and receiver sides are shown in Fig. A.8. The ringing duration time is over ten times longer than the transmitting pulse width (e.g, Fig. A.7 (i) and Fig. A.8 (i)).

Received Waveforms for LPDA

The received waveforms using the LPDAs both the transmitter and receiver sides are shown in Fig. A.9. The ringing duration time is over ten times longer than the transmitting pulse width (e.g, Fig. A.7 (i) and Fig. A.9 (i)).

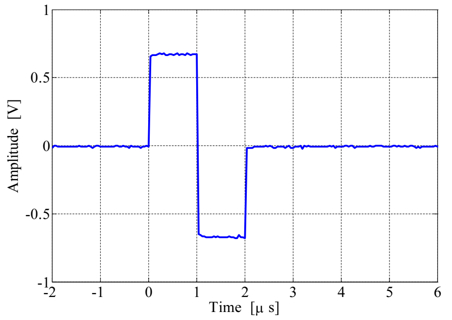

(a) 2 μs

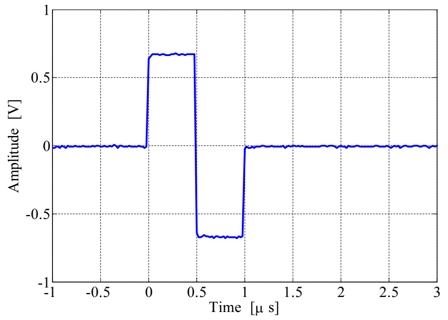

(b) 1 μs

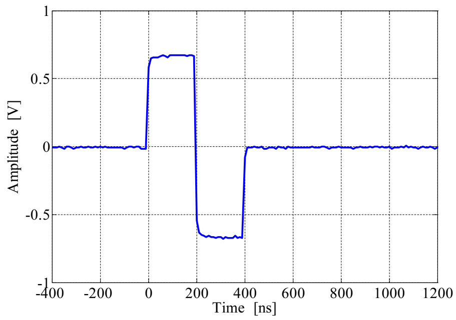

(c) 400 ns

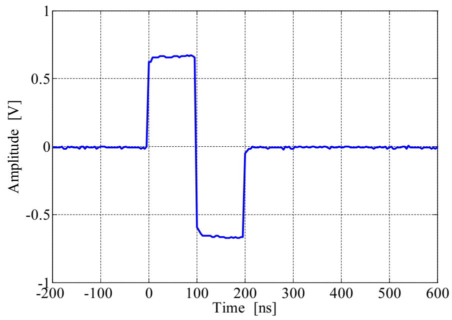

(d) 200 ns

Fig. A.7 Transmitting waveforms

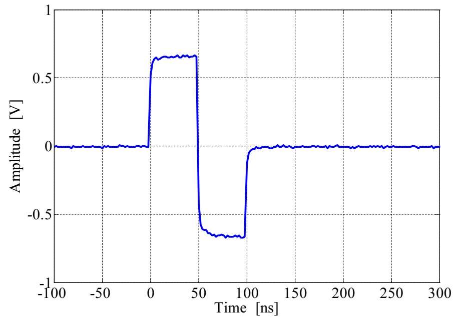

(e) 100 ns

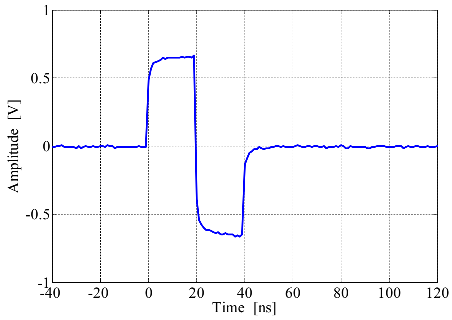

(f) 40 ns

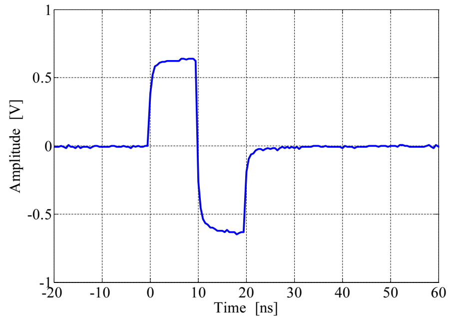

(g) 20 ns

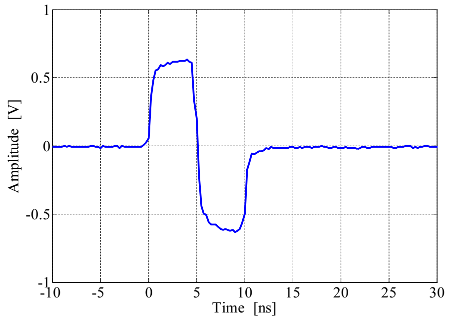

(h) 10 ns

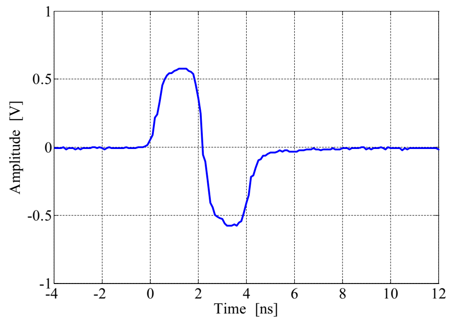

(i) 4 ns

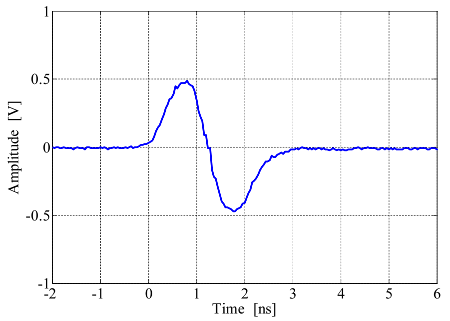

(j) 2 ns

Fig. A.7 Transmitting waveforms

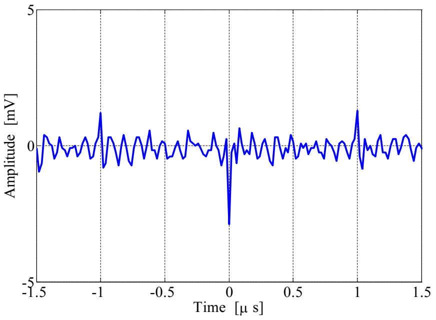

(a) 2 μs

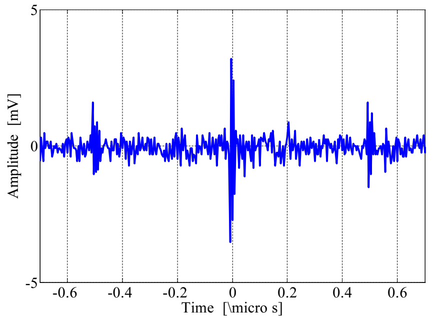

(b) 1 μs

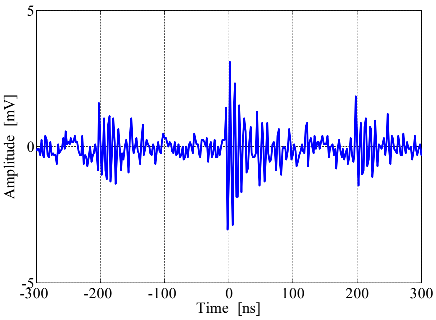

(c) 400 ns

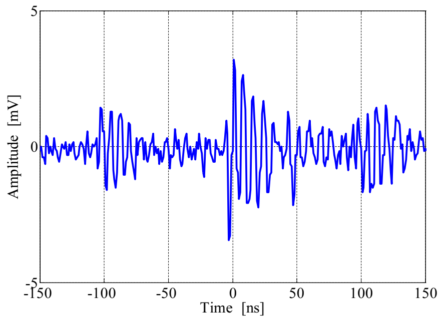

(d) 200 ns

Fig. A.8 Received waveforms for dipole antenna

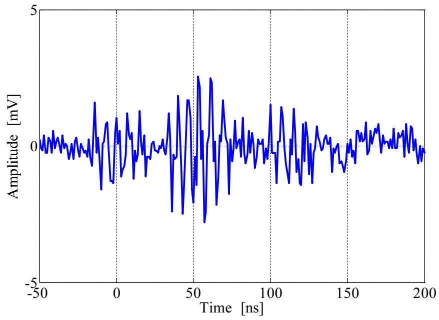

(e) 100 ns

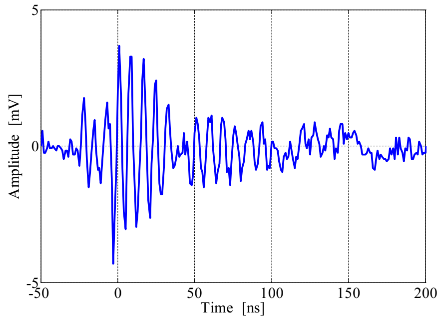

(f) 40 ns

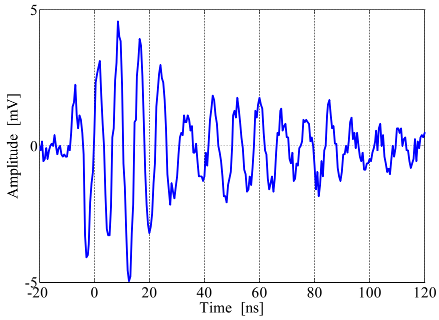

(g) 20 ns

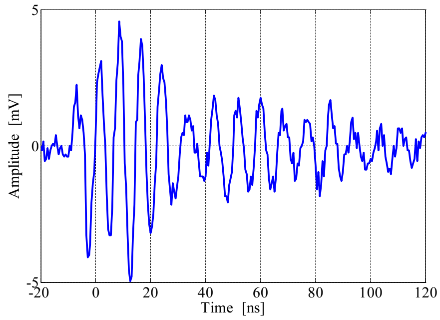

(h) 10 ns

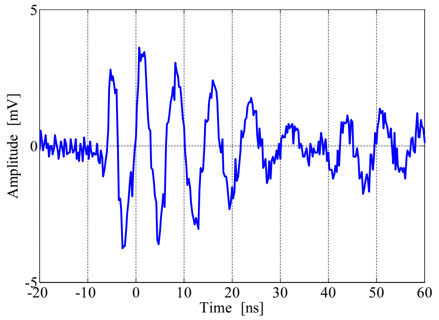

(i) 4 ns

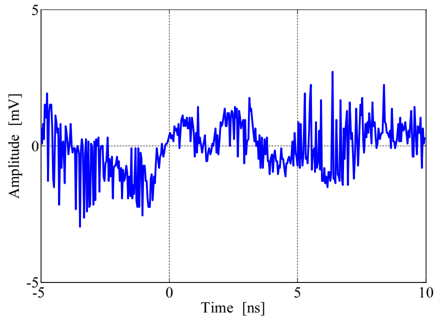

(j) 2 ns

Fig. A.8 Received waveforms for dipole antenna

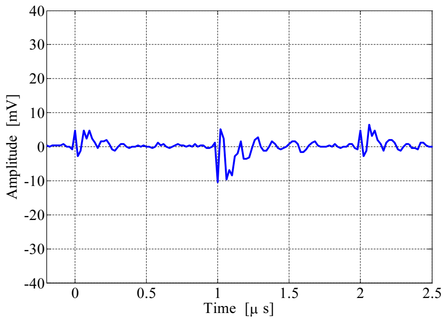

(a) 2 μs

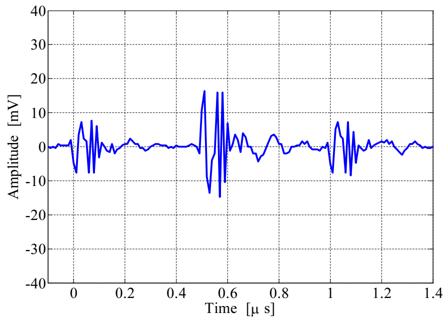

(b) 1 μs

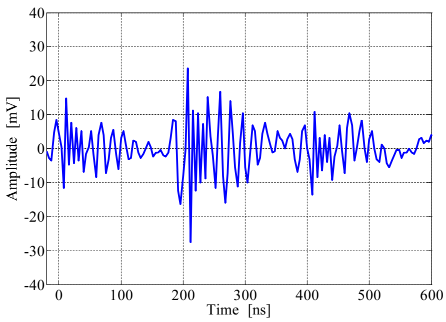

(c) 400 ns

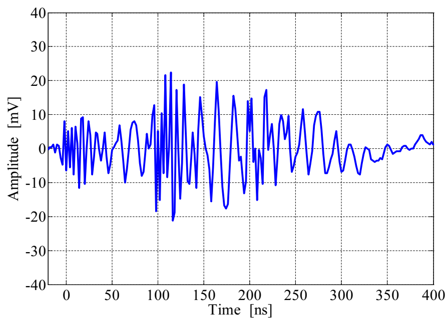

(d) 200 ns

Fig. A.9 Received waveforms for LPDA

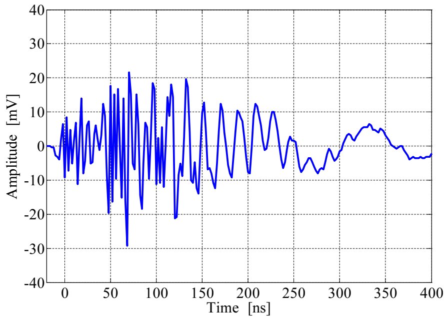

(e) 100 ns

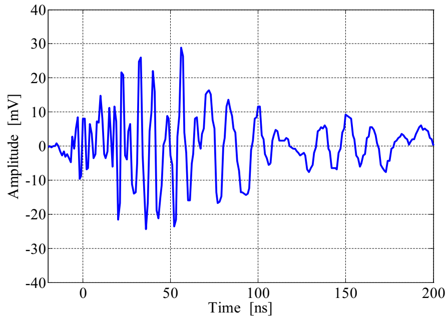

(f) 40 ns

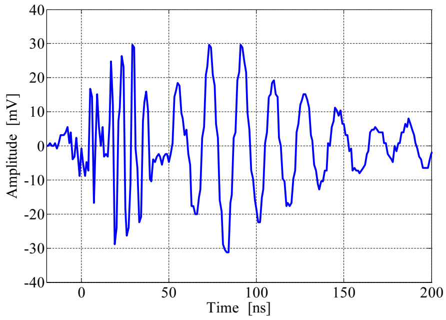

(g) 20 ns

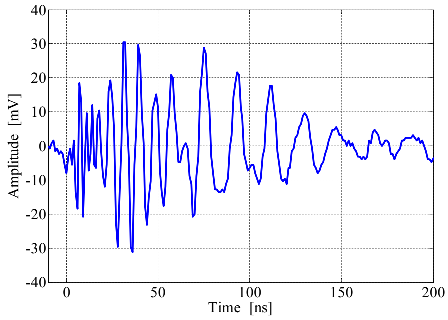

(h) 10 ns

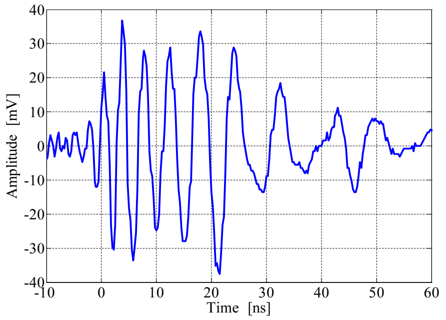

(i) 4 ns

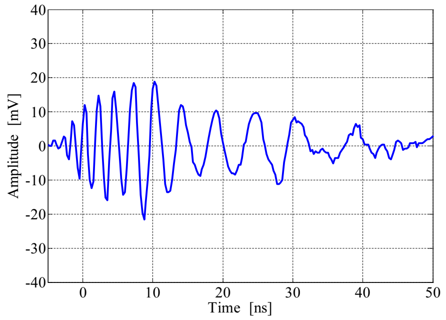

(j) 2 ns

Fig. A.9 Received waveforms for LPDA

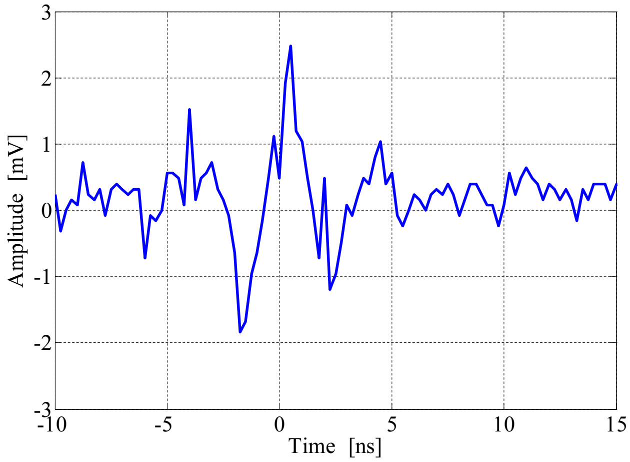

Fig. A.10 Received waveforms for resistive-loaded dipole antenna (4 ns)

Received Waveforms for Resistive-Loaded Dipole Antenna

The received waveforms using the resistive-loaded dipole antennas both the transmitter and receiver sides are shown in Fig. A.10. The received voltage could only measured at 4 ns; i.e., sufficient energy was not transmitted in other pulse widths.

A.5 Ringing in a Dipole Antenna

Some ringings are observed in a dipole antenna as shown in Fig. A.4 and Fig. A.8. This phenomenon is due to the fact that electric charges, which are driven from a DG, go along with the antenna element and repeat this act as shown in Fig. A.11

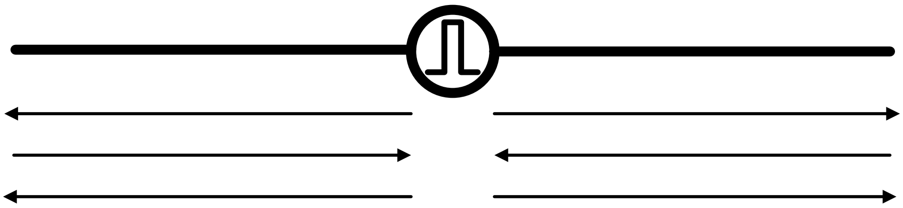

Fig. A.11 Ringing in a dipole antenna

A.6 Long Time Ringing in LPDA

In the LPDA, a longer ringing than in the dipole antenna is observed as shown in Fig. A.5 and Fig. A.9. This effect is caused by two effects. One is a ringing by the dipoles itself as mentioned in A.5, and the other is to be moved the phase centre as shown in Fig. A.12. Therefore, the phase characteristic is not linear. Assuming that the propagation lengths of lower and higher frequency components are d_{f_l} and d_{f_h}, respectively then,

$$d_{f_l} = B + L + B = 2B + L$$
$$d_{f_h} = H. \tag{A.1}$$

The difference between d_{f_l} and d_{f_h} in Eq.A.1 makes the phase centre change.

A.7 Summary

When we use such antennas dipole and LPDA, a long ringing is measured at receiver side. This means that ISI problems will occur in actual communications. Although LPDA is known as a wideband antenna, it is not suitable for WBT. Because its phase characteristic is not linear. WBT need, therefore, an antenna with wideband amplitude characteristics and wideband phase ones.

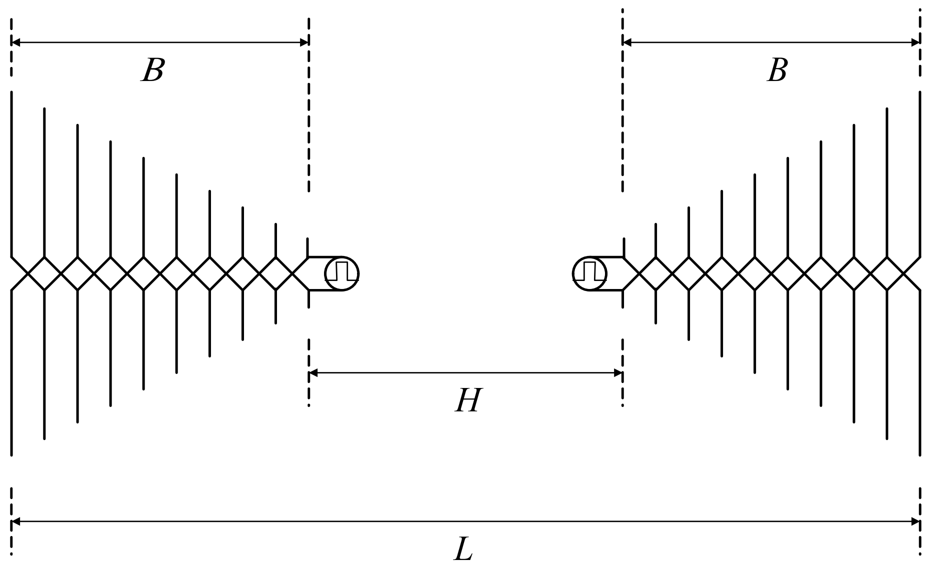

Fig. A.12 Ringing in LPDA

Acknowledgements

The author thanks Prof. Yoshio Karasawa and Dr. Tetsuki Taniguchi for their continuous encouragement for this work. The author also thanks Prof. Takeshi Hashimoto, Prof. Masashi Hayakawa, Prof. Takashi Iwasaki, and Prof. Kazuhiko Honjo for this dissertation committee.

The author is grateful to my parents. My university life for nine years and nine months had been supported by my parents Mr. Kimikazu Kitagawa and Ms. Machiko Kitagawa.

Author Biography

Jun-ichi KITAGAWA was born in Osaka, Japan, in 1978. He received the Bachelor's degree of Interdisciplinary Science and Engineering from Shimane University, Shimane, Japan, in 2001, and the Master of Engineering's degree from the University of Electro-Communications (UEC), Tokyo, Japan, in 2003. He is currently a doctoral student. He had studied the precipitation synthetic aperture radar (PSAR) at Shimane University and he is studying the wireless baseband transmission (WBT) at present. He is a first-class radio operator for general services.

Papers Related to the Thesis

1. J. Kitagawa, T. Taniguchi, Y. Karasawa, “Wireless baseband transmission experiments,” IEICE Trans. Commun., vol.E89-B, no.6, pp.1815–1824, June 2006.

2. J. Kitagawa, T. Taniguchi, Y. Karasawa, “Transmission characteristics of the wireless baseband transmission under multipath environments using real-valued signal analysis,” IEICE Trans. Electron., vol.J89-C, no.12, pp.1066–1078, Dec. 2006 (in Japanese).

Wireless Baseband Transmission – Proposal and Experiments of a New Wireless Transmission Scheme

Jun-ichi Kitagawa 2006